TVVR 16/5015

Nearshore Currents in South-eastern Scania

Emanuel Schmidt

Division of Water Resources Engineering
Department of Building and Environmental Technology
Lund University

Nearshore Currents in Southeastern Scania

Master Thesis

Author:
Emanuel Schmidt

Supervisors:
Magnus Larson
Caroline Fredriksson

LUND
UNIVERSITY

Division of Water Resources Engineering
Lund University
Box 118
221 00 Lund, Sweden

Water Resources Engineering
TVVR-16/5015
ISSN 1101-9824

Lund 2016
www.tvrl.lth.se

Master Thesis
Division of Water Resources Engineering
Lund University

English Title:	Nearshore Currents in Southeastern Scania
Author:	Emanuel Schmidt
Supervisors:	Magnus Larson, Caroline Fredriksson
Examiner:	Hans Hanson
Language:	English
Year:	2016
Keywords:	Nearshore currents; drifters; rip currents; beach morphology; swimming safety

Acknowledgements

First of all I would like to thank my supervisors Magnus Larson and Caroline Fredriksson for great enthusiasm regarding my project. You have been very kind, helpful and inspiring throughout my work with this thesis. I have had many good days of field work combined with surfing. I would also like to thank Max Radermacher from TU Delft for valuable input, useful tools and field work assistance in cold Baltic water.

Further, I would like to thank the institution of TVRL for housing me, inviting me to floor ball and for many cups of coffee. It has been a great time working with the institution and I hope to see all of you again.

Last but not least, I would like to thank my girlfriend Nína for enduring all my endless hours of explaining rip currents and numerical models instead of discussing baby names.

Abstract

The South East Coast of Scania is a popular destination for both Swedish and foreign tourists. The long and wide sandy beaches are well visited by swimmers and beachgoers, but the waters have shown to be treacherous at times. In August 2015, two German tourists drowned after getting caught in a probable rip current in the proximity of Haväng beach. Six months after the accident, this thesis study, which aims to investigate the nearshore currents in the region was initiated. The main objective was to map the currents prevalent in the area, with special attention to the offshore directed rip currents. In order to accomplish this, GPS-equipped drifters were developed for in-field measurements.

The field work includes both drifter measurements and grain size sampling. Data of the local bathymetry from the project *Skånestrand* was studied and a bathymetric survey was conducted. The study also includes offshore wave hindcasting and modeling of the wave transformation as waves approach shore.

Drifter measurements were conducted on four beaches at varying wave conditions. On 17-18 September 2016, rip currents were observed at Vitemölla beach. The offshore velocity of the current was found to be 0.4-1 m/s, which resembles velocities found in earlier studies (Winter et al. (2011), Dalrymple et al. (2011), Short (1985)). The other field measurements did not register any significant rip currents but rather strong longshore currents. The results from the wave transformation EBED model (with hindcasted waves as input) showed that a wave height variation along Vitemölla beach of more than 0.5 m can occur under the similar wave conditions. It was concluded that this could generate enough wave setup variation to drive rip currents. Furthermore, it can be concluded that most of the beaches within the study area are very dynamic, and in order to predict the nearshore currents with models up-to-date bathymetry and more reliable wave data is needed.

With field measurements, literature studies and documentation of historical accidents as a basis, a current map for the study area was developed. This study showed that the public should be attentive when swimming in the ocean when the beaches are subject to waves. A simple measure for preventing further accidents would be to red-flag all beaches under such conditions.

Contents

1 Introduction

1.1 Background

In August 2015 a tragic drowning accident occurred at Haväng beach in eastern Scania, where two German tourists were pulled offshore, caught by a probable rip current (Helsingborgs Dagblad, 2015). The existence of strong offshore directed currents on the southeast coast of Scania is widely known among local residents and warning signs have been placed on the beaches to notify swimmers about the strong currents. However, the processes generating the currents are poorly understood and has not previously been studied in the area. This master thesis focus on studying the nearshore currents along the southeast coast of Scania and their basic characteristics.

Understanding the nearshore hydro- and morphodynamic processes can help to predict where and when currents are formed. Identifying the conditions under which currents may occur is valuable to educate the public and may form the basis for a warning system to prevent further accidents.

1.2 Research Questions and Objectives

The main objectives of this study is (1) to map the nearshore currents along the southeast coast of Scania, (2) to determine the underlying mechanisms and (3) to quantify their basic characteristics. This thesis aims to answer the following research questions:

- What types of currents occur along the coastline?
- Along which parts of the coastline in the study area do rip currents occur?
- Under which wave conditions do rip currents occur?
- How is beach morphology coupled to currents?
- How can knowledge about nearshore currents be used in coastal- and safety management in southeast Scania?

Based on an initial investigation, some beaches will be chosen as field study sites for which the following research questions will be investigated:

- What is the rip cell morphology?
- How strong is the rip current?

1.3 Methodology

The study is divided into five main parts: 1) a literature study, 2) mapping of nearshore current conditions, 3) construction of drifters 4) field measurements, and 5) data analysis.

1.3.1 Literature Study

International literature on nearshore currents is abundant, but most studies have been carried out at swell dominated coastlines. However, a few studies have been carried out at coastlines dominated by wind waves (e.g., Winter, 2011). The focus of the literature study was to gain understanding of the physical processes of nearshore currents (especially rip currents) and other offshore directed currents, how they interact with beach morphology, and under which wave and morphological conditions they are likely to occur. The literature review also encompassed previous studies where field work has been performed as a preparation for the measurements to be carried out in the present study.

1.3.2 Mapping of Rip Current Conditions

Based on the conceptual understanding of nearshore current formation, a mapping of current conditions was undertaken. The mapping was mainly based on the material about beach morphology collected by the Swedish Geological Survey (SGU) in the project Skånestrand (Persson et al., 2014). The bathymetry data from the project is classified and a qualitative study of rip current indicators was partly conducted during a study visit at SGU in Uppsala. Furthermore, the deep water wave climate was calculated based on wind data from the Swedish Meteorological Institute (SMHI) and bathymetry from EMODnet, using the SPM-method modified with a memory function according to Hanson and Larson (2008). Existing observations of strong currents in the area were compiled from the municipalities (Ystad and Simrishamn), lifeguard organizations, local surfers and fishermen.

1.3.3 Construction of Drifters

In order to collect data, simple, low-cost drifters were constructed with inspiration from existing products and earlier studies. The type of GPS used is relatively cheap (intended for outdoor use) and weatherproof. The drifter material used can be found in any regular hardware store.

1.3.4 Field Measurements

Based on result from the mapping, four beaches were chosen for a more detailed study of the hydro- and morphodynamic conditions. The field study includes grain size sampling, bathymetric survey by RTK-GPS and current tracking with drifters.

1.3.5 Data Analysis

Collected data was analyzed in order to relate current properties to the wave conditions and the beach morphology. The wave transformation model EBED was set up for a location and the output was analysed.

1.4 Thesis Structure

Chapter 1 - Introduction includes a short background to the choice of thesis, the main research questions and objectives. The methodology explains how these questions will be encompassed.

Chapter 2 - Theoretical Background describes the theoretical findings from literature studies. It covers relevant ocean processes; wave generation, refraction, shoaling and diffraction, wave setup, infragravity waves, nearshore currents and beach morphology.

Chapter 3 - Description of Study Area explains the local conditions at the study site, including both bathymetry and wind/wave climate.

Chapter 4 - Drifter Development describes the process of developing GPS-equipped drifters for field measurements.

Chapter 5 - Field Measurements describes the methods used in field experiments; bathymetry measurements, grain size sampling and drifter experiments.

Chapter 6 - Field Measurment Results presents field experiments findings; grain size sampling, bathymetrical surveys and drifter current tracking.

Chapter 7 - Modeling includes model setup, input data, results from modeling with EBED and simple current calculations.

Chapter 8 - Discussion consists of five parts: drifter experiment, morphodynamics, data analysis, safety recommendations and further research recommendations.

Chapter 9 - Conclusions summarizes the findings from the project.

2 Theoretical Background

Nearshore currents is a field that has caught coastal researchers attention for many decades and there are plenty of studies covering the physics behind them. The characterization of near shore currents started already in the 1920's in *Science* and it is not yet a closed chapter (Davis, 1925). This theoretical background will guide the reader through parts of the physics that induce nearshore currents, starting with wave generation. This introduction to hydrodynamics is helpful to understand the following chapter which describes what types of currents that can be found on a beach. As no beach is the other one alike, the conditions forming current systems are unique from beach to beach. A cornerstone in understanding the dynamics of beaches and morphodynamic processes that form and change them is the extensive work of Wright and Short in the 1970-1980s. Thus, the Beach State Classification that was defined by these pioneer researchers will also be presented to the reader in this chapter.

2.1 Ocean Waves and Nearshore Transformation

Waves generated by wind is generally the largest energy input to coastal systems and therefore the wave climate on a beach is the singlemost important parameter determining the morphology and the nearshore currents. As waves approach shore they undergo transformation where the energy in the waves is redistributed. These mechanisms are described in the two following subchapters.

2.1.1 Wave Generation

Waves are generated by transfer of energy from the wind to the sea. The wave height is limited by following parameters:

- Wind (speed, direction and duration)
- Fetch, the distance over which the wind is acting. It can either be limited by the wind field (meteorological fetch) or by the water area (geographical fetch).
- Water depth at the area where the waves are formed.

Waves that still are under influence of wind forces are steep and of short periods, causing the surface to appear irregular. These waves are often referred to as *short-crested waves* (also *wind waves*). As the waves propagate away from the area of generation the smaller waves are attenuated and the waves line up with a longer period and a well defined trough and crest. These waves are called *swell*.

2.1.2 Refraction, Shoaling and Diffraction

The speed at which a wave propagates is called wave celerity, C, and depends on the gravity g, the wavelength L and water depth d as:

$$C = \sqrt{\frac{gL}{2\pi} tanh\left(\frac{2\pi d}{L}\right)} \tag{1}$$

From Equation 1 it can be seen that when the water depth decreases, the wave slows down. Wave frequency do not change and therefore the wavelength decreases with decreasing celerity. To maintain the energy flux, a decrease in celerity is compensated by an increase in energy density causing the wave height to increase. This process is called *shoaling*. As waves approach shore, the part of the wave that first reaches the shallower water will slow down, causing the wave to bend and align with the bottom contours. This phenomena is called *refraction*, see Figure 1.

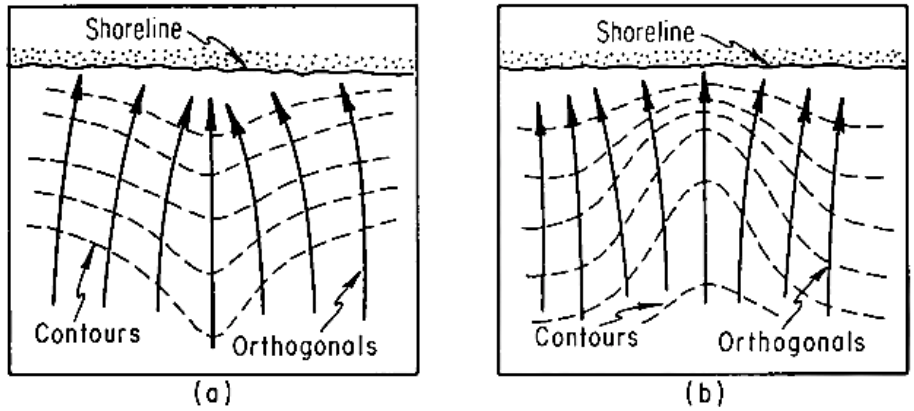

Figure 1: Refraction by a) a submarine ridge and b) a submarine canyon. (U.S. Army Corps of Engineers, 1984)

Refraction can also occur due to current-wave interaction, where the current slow down the waves. Another important phenomena that alters the wave height is *diffraction*. When a wave passes an obstacle, such as an island, the energy is transported laterally along the wave crest towards the shaded area, causing the wave to bend after passage. Diffraction therefore simply redistributes energy and superimposition of diffracted incident waves causing wave height variations behind the obstacle. All these phenomena are of great importance when discussing

the formation of nearshore currents as they contribute to alongshore variation in *wave setup*.

2.2 Wave Setup

Wave setup is the superelevation of mean water level caused by wave action. It is not to be mixed up with the elevated water levels that derives from storm surges (wind setup). The phenomena of wave setup was discussed already in the 1960's and through field- and laboratory studies the magnitude of the setup was found to elevate the water level by 10-20% of the incident wave height (Dean and Walton, 1990). The wave setup is often denoted as η and the total water depth, d, is the sum of still water depth, d_s and this mean surface elevation η:

$$d = d_s + \bar{\eta} \tag{2}$$

When waves travel towards shore they convey both energy and momentum and as the waves break, the energy is dissipated which can be observed by the increased turbulence in the white water. The wave-related momentum on the other hand is transferred to the water shoreward of the breaker point. To balance the onshore component of the flux of momentum, a slope of the water surface develops as seen in Figure 2 (MWL).

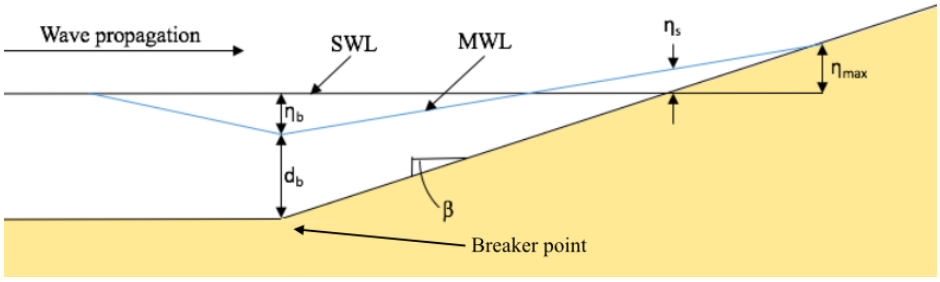

Figure 2: Wave setup on a uniformly sloping beach. The still water level (SWL) is defined as the water level without influence of wave action. The mean water level (MWL) on the other hand includes this factor and is defined as the average water level with respect to temporal fluctuations.

Longuet-Higgins and Stewart (1964) thoroughly described the physics behind the wave setup as follows. For normally incident waves, the mean water level slope can theoretically be described as:

$$\frac{d\eta}{dx} = -\frac{1}{\rho g d}\frac{dS_{xx}}{dx} \tag{3}$$

where ρ is the water density and g is the gravitational constant. S_{xx} is the flux of momentum in the x-direction by the x-component of momentum. When assuming longshore and homogenous waves and bathymetry it can be stated as:

$$S_{xx} = E\left[\frac{2kd}{sinh(2kd)} + \frac{1}{2}\right] \tag{4}$$

where E is the total wave energy density, including both potential and kinetic energy of the wave:

$$E = \frac{1}{8}\rho g H^2$$

where H_b is the breaking wave height. Assuming shallow water and linear wave theory, S_{xx} can be simplified to:

$$S_{xx} = -\frac{3}{16}\rho g H^2 \tag{5}$$

By integrating the setup slope in Equation 3 assuming linear wave theory, normally incident waves and no setup in deep water, the setdown outside the breaker zone becomes equal to:

$$\eta = -\frac{1}{8}\frac{H^2 k}{sinh(2kd)} \tag{6}$$

where k is the wave number at breaking ($2\pi/L$). By combining Equation 3 and 5, the gradient is given by:

$$\frac{d\eta}{dx} = -\frac{3}{16}\frac{1}{d}\frac{d(H_b^2)}{dx} \tag{7}$$

The value of η depends on the wave decay through the surf zone. With a saturated breaker assumption, meaning essentially all waves are breaking, the slope of the water surface is given by:

$$\frac{d\eta}{dx} = -\frac{1}{1 + \frac{8}{3\gamma_b^2}} tan\beta \tag{8}$$

where tan β is the beach slope. The breaker depth index, γ_b, is given as the relation between offshore wave height and bottom slope. The setup at the beach interception with the still water level, η_s is then found by assuming setdown at the breaker point and combining Equations 6 and 8 gives:

$$\eta_s = \eta_b + \left[\frac{1}{1 + \frac{8}{3\gamma_b^2}}\right] h_{s,b} \tag{9}$$

where $h_{s,b}$ is the breaker depth ($d_b + |\eta_b|$) and η_b is the setdown at the breaker point:

$$\eta_b = -\frac{\gamma_b^2 d_b}{16} \tag{10}$$

Variations in wave height along the beach, caused by e.g. submarine canyons or man-made jetties will lead to a varying wave setup along the beach. This water level variation therefore to a large extent determines the flow conditions in the water close to the beach. These above given equations can be used in numerical calculations of the driving forces for nearshore currents, but it is important to remember that it is simplified and under several assumptions.

2.3 Flux of Momentum Under Oblique Waves

The momentum balance (Equation 4) can also be written as:

$$S_{xx} = E\left[n(cos^2\theta + 1) + \frac{1}{2}\right] \tag{11}$$

where n is the ratio of wave group velocity to wave celerity and θ is the wave angle towards the normal of the beach (Olsson, 2004). It can be seen from Equation 11 that momentum flux in the x-direction is maximum for $\theta = 0°$. To estimate the momentum losses for oblique waves in shallow water, Dean and Walton (1990) did a simple numerical calculation and found that the reduction of momentum flux in the x-direction is 16,7% for a wave angle of 30°. This could imply that even if waves have an oblique angle towards shore, the driving force for offshore directed currents is still relatively large.

2.4 Infragravity Waves

It is believed that interaction between *infragravity waves* and incident waves can create currents as it affects the mean water level. Infragravity waves are surface gravity waves with periods longer than wind waves (more than 25s). Generally, these waves can be divided in three categories: 1) bound long waves, 2) edge waves and 3) leaky waves. Bound long waves originate from the wave height variation found within a wave group. The larger waves in a wave group will cause the setup to temporally increase and when smaller waves reach the shore, the setup will consequently decrease. This oscillation is thus of the same frequency as incident wave groups. Edge waves are freely propagating waves originating from wave reflection at the shoreline. The edge waves are trapped inside the breaker zone, with an antinode on the beach and an exponential decay of the amplitude seaward. These waves have been found to be one reason for the formation of rhythmic longshore variations of the beach face; beach cusps (Guza and Inman,

1975) (beach cusps can be seen in Figure 5.3-5). Leaky waves also originate from shoreline reflection but just like long bound waves they are freely propagating or standing waves and they are not trapped by the bathymetry like edge waves.

2.5 Nearshore Currents

The nearshore currents in two dimensions can be described by following momentum- and continuity equations by Olsson (2004), which are valid for depth-averaged, steady-state conditions. The momentum equation for nearshore currents include the wind and wave forcing, pressure gradients due to wave setup, lateral mixing of the water masses and bottom friction.

$$\begin{cases} U\frac{dU}{dx} + V\frac{dU}{dy} = -g\frac{d\bar{\eta}}{dx} + F_{bx} + L_x + R_{bx} + R_{sx} \\ U\frac{dV}{dx} + V\frac{dV}{dy} = -g\frac{d\bar{\eta}}{dy} + F_{by} + L_x + R_{by} + R_{sy} \end{cases}$$

And the continuity condition is:

$$\frac{d(Ud)}{dx} + \frac{d(Vd)}{dy} = 0 \tag{12}$$

where U and V are the velocities of the cross-shore and longshore currents. The water level gradient due to setup, $\frac{d\bar{\eta}}{dx}$ is defined by Equation 8. F_b is the bottom friction component which is a resisting force to the currents. L is the component of lateral mixing which tends to smoothen out the effects of wave forcing, R_b. Finally R_s is the component of wind forcing. (Olsson, 2004)

The main parameter that determines the strength of nearshore currents are radiation stress from breaking waves. Radiation stress can be defined as the excess flow of momentum due to the presence of the waves (Longuet-Higgins and Stewart, 1964). Although, wind stress with an angle from the normal to the beach also largely affects nearshore current velocities (Hubertz, 1986).

2.5.1 Longshore Currents

Longshore currents are nearshore currents that flow parallel to the shoreline and extend throughout the surf zone (the zone of breaking waves) to rapidly decrease outside the breaker. The currents are generated by radiation stress from wave and wind action and typical velocities are 0.3 m/s, but during storms they can reach speeds over 1 m/s (Visser, 1991). Longshore currents can also be driven by a pressure gradient from wave setup and thus be generated by alongshore variations in wave height (Olsson, 2004). Analytical solving of the momentum

and continuity equations described in the previous chapter is often non-trivial and time demanding. A simplified expression for longshore current velocity, V, assuming homogeneity in the longshore bathymetry, linear wave theory, saturated wave breaking, no lateral mixing and small wave breaking angle was derived by Longuet-Higgins (1971) (as cited in U.S. Army Corps of Engineers (2002)):

$$V = \frac{5\pi}{16} \frac{tan\beta^*}{C_f} \sqrt{gd}\, sin\alpha\, cos\alpha \tag{13}$$

where $tan\beta^*$ is the beach slope considering wave setup (Equation 8), C_f is the bottom roughness (typically 0.005 - 0.01) and α the angle between the incident waves and the bottom contours.

2.5.2 Undertow

Undertow is a return flow of water that has been carried shoreward by waves. According to linear wave theory, the motion of the waves is completely oscillatory, but observations and more advanced analysis show that the particle orbits are not completely closed. Every time a wave passes, there will be a net mass transport of water in the direction of propagation. (U.S. Army Corps of Engineers, 1984) The beach can be considered as a solid boundary and thus the water transported shoreward needs to be carried back towards the surf zone to satisfy the continuity condition. This return flow often appears as a laterally homogenous near bed current, undertow. The currents are generally most prevalent during high wave energy conditions on low-sloping beaches and the mean offshore velocities can reach 0.5 m/s (Aagaard and Vinther, 2008). The magnitude of the undertow depends upon the steepness of the breaking waves but other currents (like rip currents) can also distort the strength of the undertow (Olsson, 2004).

Before the different nearshore currents were thoroughly studied there was large confusion in naming the different currents. For many years, undertow was synonymous with rip currents (see next chapter *Rip Currents*). Today the distinction between these two currents is clear amongst coastal researchers, but in the public, the terminology is often mixed up. For example, the warning signs at the coast of Scania still uses the term "undervattensströmmar" (directly translated "under-water currents") for hazardous currents.

2.5.3 Rip Currents

Just like undertow, rip currents are a return flow of water transported shoreward by wave action. Rip currents are strong, often narrow currents, flowing seaward perpendicular to the beach. The currents are one of the worlds most lethal natural hazards and it can carry swimmers of all abilities to deeper water in minutes

(Dalrymple et al., 2011). Rip currents have been discussed and researched for several decades and early studies by Bowen (1969) showed that the strength and the seaward extension of the currents is related to the incident wave height.

As discussed in chapter *Wave Setup*, wave action on a beach will cause wave setup on the shoreward side of the bars. In areas where the bar is less accentuated and depth is greater, the influence of wave action on the setup will decrease. The water level variations inside the bars will give rise to a hydraulic head which induce longshore currents towards zones with less setup. Where these longshore currents converge, a narrow, seaward directed rip current forms, see Figure 3. Outside the surf zone the driving forces for the current rapidly weakens and the current ceases. Under certain conditions (mostly under normal incident waves) a circulation cell is formed where the water parcels move in a semi-closed loop.

Formation of rip currents therefore depends on a longshore variation in wave height. There are several processes that can lead to a varying wave height, for example refraction due to irregular bathymetry and diffraction due to headlands or structures (Dalrymple, 1978). Bowen (1969) also discussed that wave height variations can arise from wave-wave interaction between edge waves and incident waves. Furthermore, tidal variation is an important parameter that determines the occurrence of rip currents, where low tides generally generate more and faster rips (MacMahan et al., 2006).

Shepard et al. (1941) visually identified three major features of a rip current; the feeder, a longshore current that converge in the areas with less setup, the rip neck, a narrow channel of fast seaward directed flow and the rip head where the current diverge and the velocities decrease. This is schematically presented in Figure 3.

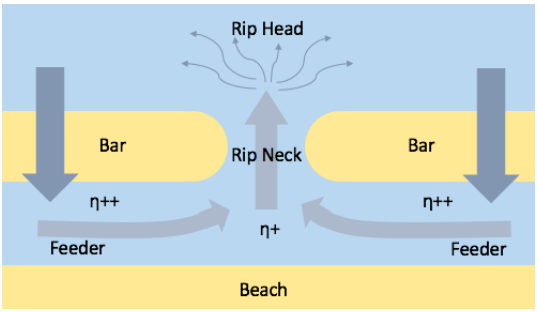

Figure 3: Schematic view over rip current formation on a beach with longshore bars. $\eta+$ means little or no setup while η^{++} indicates high setup.

The seaward flow in rip currents can often be visually identified as darker regions in between regions of white, breaking waves. This can be seen in Figure 4b. In areas with fine sediment they can also be spotted as brownish patches of suspended material. Even for someone with great experience, rip currents can be very difficult to identify as they attain many shapes, from stationary mega-rips to short-lived leaky flows. Dalrymple et al. (2011) listed and described the present knowledge about rip currents and here follows a summary of these rip current types and their morphological characteristics.

The most commonly discussed types and most easily observed are the alongshore linear bar-trough with incised rip channels (Figure 4a) and the transverse bar system (Figure 4b). If a longshore current, originating from obliquely incident waves, is interrupted by a jetty or groin the water level along the obstacle increases, creating a hydraulic head that can cause an offshore flow. Such rip currents (Figure 4c) are present on almost all beaches with coastal structures or headlands and the currents are often utilized by surfers to cross the surf zone with less effort. On beaches enclosed by headlands (pocket beaches) strong, wide mega-rips can develop in the center of the beach which often extend longer offshore than on open beaches (Figure 4d). All these types of currents are morphologically controlled (except 4c), that is they depend on the bathymetry. The last type of common seaward flowing currents are the transient rips (Figure 4f-g). Transient rips are often found in combination with strong, meandering longshore currents which tend to "leak" offshore.

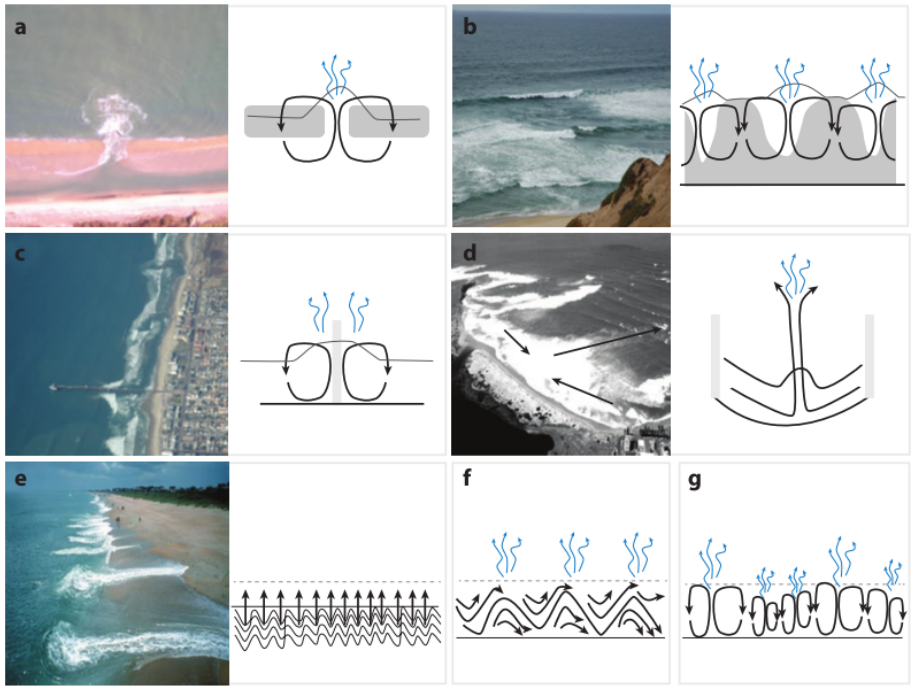

Figure 4: Different types of rip currents as described by Dalrymple et al. (2011).

Rip current channels have occasionally been found to be stationary but on open beaches they tend to migrate alongshore (Aagaard and Vinther, 2008). Once a bar-channel bathymetry is formed, the current is bathymetrically forced and can persist at the same locations until the wave conditions change (Short, 1985). The spacing between rip currents is not fully understood but they tend to appear at a distance of 50-1000 m on open beaches (Holman et al., 2006; Huntley and Short, 1992) as cited in (Aagaard and Vinther, 2008). The mean velocity of rip currents are typically 0.2-0.7 m/s but during storms they have shown to reach speeds above 1 m/s (Shepard and Inman, 1950). MacMahan et al. (2006) examined historical rip current experiments and discussed that rip currents have a low average cross-shore velocity with stronger velocity maxima on a rather short time scale. The temporal variation with stronger maxima was found to be at a time scale of 25-250 s which corresponds to wave group frequency.

2.5.4 Backwash

Another type of shore perpendicular current that is often mistaken for rip currents are swash rips (often referred to as backwash) (Figure 4e). On beaches with coarse sediments where a steep foreshore has developed, the waves break close to the beach face. The surf zone on these beaches is often short and waves often break as plunging waves. The waves run up on the beach face with high velocities and the return flow, which at times can be violent, is called backwash. This current is unlike the previously described (except rip current around structures, (Figure 4c)) primarily driven by gravitational forces. (Davidson-Arnott, 2010) Since the current do not extend far offshore, it is not capable of carrying a person far out. On the other hand they can be hazardous to beachgoers as they are related to steep wave breaking.

2.6 Beach Morphology and Storm Response

Sandy beaches are the most dynamic systems within the nearshore region and it is here that most of the energy from waves is dissipated. The beach adjusts its profile to efficiently encounter the incoming waves and therefore a beach can look surprisingly different from one time to another. As discussed in the chapter of wave setup, the wave energy is dissipated as the wave break; turbulence is generated and sediment is lifted and moved. As a rule of thumb, a wave breaks at a depth of about 1.2 times the wave height and where the wave breaks therefore depends on the nearshore slope. After breaking the wave can reform to break again further towards shore to finally dissipate the last energy as the wave rush up on the beach face. If the wave energy is increased the beach often responds by transporting sediment seaward to form a bar. This allows wave breaking at a longer distance from shore, widening the surf zone and reducing the wave impact on the beach face. As storms with large and steep waves hit the coast, the beach response is often drastic. Storms are often related to onshore winds which generates an elevated water level, a storm surge. This surge allows the waves to pass the nearshore and break closer to the beach, resulting in erosion of the beach berm and sometimes even the dunes. The sediment is transported offshore and finally deposits where the turbulence is lower, forming an offshore bar. This transport is ongoing until the bar grows large enough to sufficiently dissipate the wave energy. As the wave height decreases after a storm or a season of storms, the beach and dunes start recovering to a calmer climate. Usually, the sediment is transported onshore by long period swell with low wave heights but this process takes more time than the short-lived storms that caused the erosion. The recovery process was thoroughly studied by Wright and Short (1984) and parts of their findings are presented in the next chapter.

During especially heavy storms, some of this sediment may also be transported away from the active profile and the beach can not recover to the pre-storm morphology. The erosion is then permanent causing the shoreline to retreat. As some coastlines seldom or never receive long period swells the storm recovery is extremely slow, which seemingly is the case for the Coast of Scania.

2.6.1 The Beach State Classification

The beach state classification by Wright and Short (1984) is the result of extensive studies and field measurements of beach morphodynamics at numerous Australian beaches. The field work included daily monitoring of beach transects and measurements of waves and currents within the surf zone. The broad studies led to a classification system with two extremes; dissipative and reflective beaches followed by four intermediate states. The six different states are graphically presented in Figure 5.

Dissipative beaches (1) are generally characterized by very wide surf zones with low mean slopes and multiple stable bars. This beach state generally appears after storms and is therefore often referred to as winter profile, as winters generally are stormier than summers. Longshore irregularities in this beach state are rare and the beaches function as sinks for fine sediment. Depending on the grain size, the beach face can be either flat or moderately steep (almost reflective) and thus the slopes are divided into "beach profile slope" and "inshore profile". If the beach lies in an area without major deposition sources, the first bar is generally observed at a distance of 100-200 m from shore and longshore currents form in the wide trough. Fast, narrow and widely spaced rip currents can occasionally develop over the bar on long beaches. (Wright, 1979)

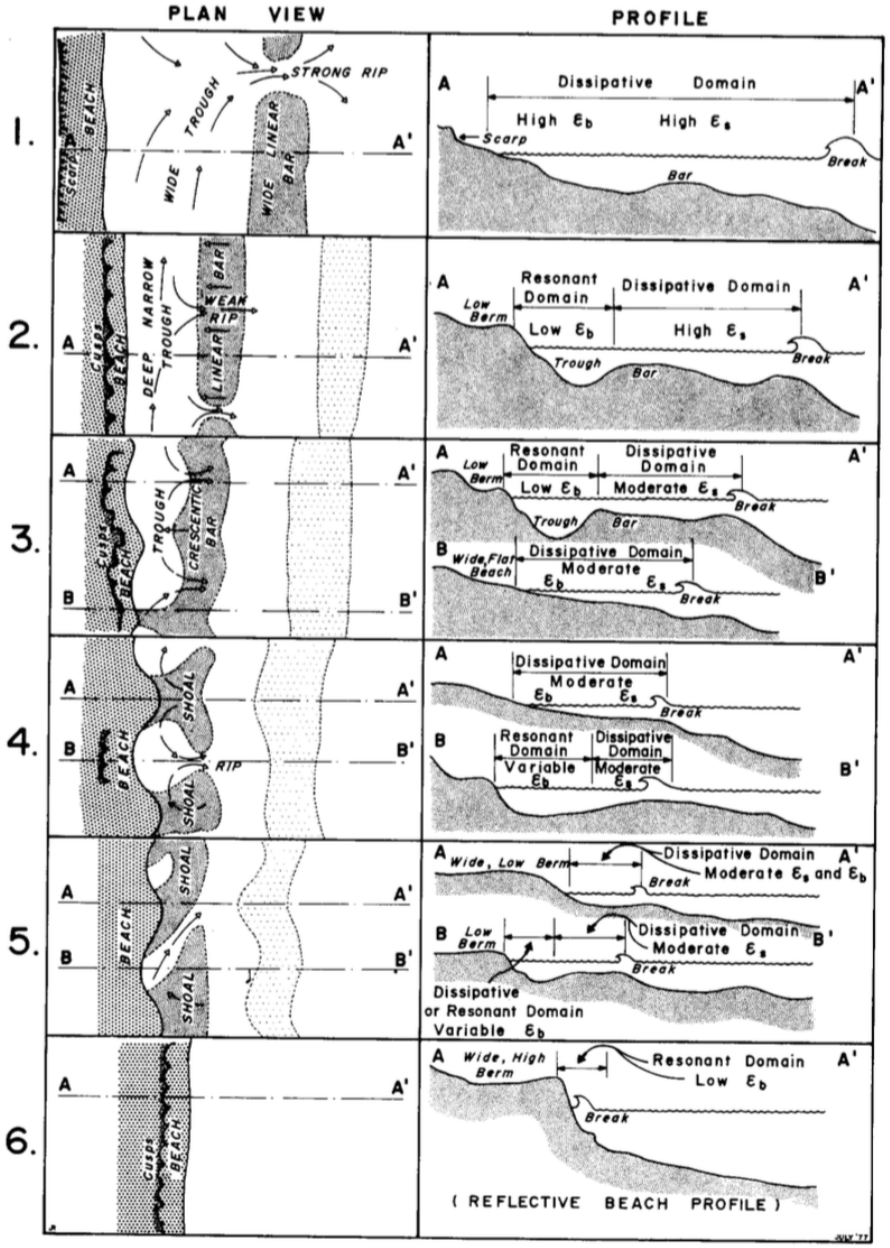

Figure 5: The six general beach states proposed by Wright (1979) with (1) being fully dissipative, (6) fully reflective and (2-5) intermediate stages.

Reflective beaches (6) on the other hand have a short surf zone with a linear steep beach face and a linear low sloping inshore. As waves approach shore they slowly shoal and finally break as surging or collapsing waves close to shore. This type of beaches are most prevalent in deep embayments or semi-protected environments. At beaches with a modest wave exposure the sediment can be fine to medium sand but at exposed beaches the sediment is coarse.

The first intermediate stage (3) appears shortly after a stormy period. Smaller waves cause the bar to migrate shoreward to 50-100 m from shore, and the trough deepens. The increased trough depth cause waves to reform and the waves break on the beach face. The beach face is partly reflective which causes beach cusps to start forming. The longshore current still feeds rip currents but the spacing between channels decrease. As a period of calm waters continue, the beach morphology continue to change; the bars move further toward shore and attain a cresentric shape to finally attach to the beach face (4). If accretion continues, a well-developed rhythmic bathymetry develops with transverse bars and deeper embayments. This morphology also induce rip currents flowing seaward from the embayments. Waves with an oblique angle can further cause the transverse bars to attain a skewed shape. The last intermediate stage (5) can be found after a long period of calm water. The wave energy is dissipated before it reaches the beach face and the sediment can settle. Rip currents usually weaken and the embayments can evolve to isolated pools.

If the accretionary processes are ongoing the wave shoaling can cause the sediment to move shoreward and increase the subaerial storage until the beach become fully reflective. On open coastlines, fully reflective beaches are rare and only form for a couple of months during periods of low wave energy and therefore this state is often referred to as the summer profile.

To classify the beaches, a modal beach state parameter Ω was developed based on breaking wave height H_b, the mean sediment fall speed $\bar{w_s}$ and the wave period T:

$$\Omega = \frac{H_b}{\bar{w_s} T} \tag{14}$$

where the settling velocity $\bar{w_s}$ could be given by for instance the empirical formula by Zhiyao et al. (2008) which is a function of the sediment radius d, the kinematic viscosity ν:

$$w_s = \frac{\nu}{d} d_*^3 [38.1 + 0.93 d_*^{12/7}]^{-7/8} \tag{15}$$

where d_* is the dimensionless particle diameter:

$$d_* = \left(\frac{\Delta g}{\nu^2} \right)^{1/3} d \tag{16}$$

It was found that reflective beaches with $\Omega \leq 1$ remain stable as reflective, and dissipative beaches remain stable as long as $\Omega \geq 6$. This means that intermediate states can begin to develop when $1 < \Omega < 6$. The classification system was mainly developed for swell-dominated beaches with large seasonal swell variation, and in the Baltic Sea the wave climate is exclusively dominated by wind waves. The beaches will therefore most often not receive any waves and Ω is not especially applicable. However, the beach state concept is useful for predicting current patterns and Dalrymple et al. (2011) conclude that rip currents are mainly found on beaches with intermediate beach states and that the intensity increases with increasing alongshore bathymetric variability.

2.7 Swimmer Safety

Stories of treacherous currents at the beaches along the southeastern Coast of Scania are found among the local residents and the municipalities warn the public through warning signs. In August 2015, a 7-year old girl unfortunately got stuck in what was believed to be a rip current and her father tried to rescue her. The father was found in the water by rescue personnel but was declared dead before arriving at the local hospital. The girl was not found until two days later, a couple of hundred meters north of the accident site (Claes Jeppson, 2016). After the accident, the municipality of Simrishamn initiated a risk assessment based on local knowledge about currents, history of accidents and number of beach visitors. Three beaches were considered to have elevated risk; Kyhl, Knäbäckshusen and Haväng (Soderberg, 2016).

As earlier discussed, there is a plethora of currents that can be hazardous for beachgoers and the current systems will differ from beach to beach. The swimmer's worst enemy is not the current itself but the panic and irrational thinking trigged by the powerful nature of the currents. Generally there are no nearshore currents that are capable of pulling people down under surface but the real danger is the exhaustion from swimming against the current. The key to safe beaches is understanding how the currents work, where they form and how to act when caught in them. Most of beach-related rescues are found on beaches where strong rip currents are present. The offshore flow easily induces stress for swimmers even though they often are quite easy to escape. Since the rip currents are relatively narrow it is recommended to swim parallel to the beach or simply relax and let the current carry the swimmer out of the surf zone, where the current disperses. Longshore currents are best dodged by swimming towards shore but when the swimmers reference point on the beach rapidly disappears, these currents are also stressful.

Since rip currents are considered to be one of the most lethal natural hazards,

several attempts have been made to forecast the occurrence of these. Most warning systems have been developed for American beaches and the number of lifeguard rescues have been compared with a wide range of parameters; wind- and swell direction and speed, wave period, tidal levels, beach state and number of swimmers. The nearshore region is a complex and constantly changing area and proposed risk forecast models have had varied success. Since there are a lot of mechanisms that can induce rip currents (such as eddies along hard structures, wave-wave interaction and transient rips in longshore currents), the models have to incorporate all these factors to predict the currents satisfactory (Dalrymple et al., 2011).

3 Description of Study Area

3.1 Study Site

The long coastline of Scania is a popular area for sport fishing, sunbathing and beachgoing and therefore several of the beaches are crowded with people during the warm summer months. The study area was limited to the beaches of Simrishamn municipality and Sandhammaren beach in Ystad municipality, covering a 45 km stretch of coastline. All sandy beaches within the study area were visited and investigated. An image of the offshore bathymetry is presented in Figure 6. The location of the beaches are presented in Figure 7. The Baltic Sea is too small to generate any tidal variation and the Strait of Öresund is too narrow to allow the Baltic Sea to be influenced by Atlantic tides. At times, tidal waves from Kattegat can have an effect on the sea level in the study area by a few centimeters (SMHI, 2010). The different beaches are subject to similar wave climate, with waves primarily propagating from the east. As mentioned in the *Theoretical Background*, the offshore bathymetry will cause the waves to transform when approaching the coast. To attain a complete picture of the wave climate, a wave hindcast model was run for the last 20 years. The findings are presented in Chapter *Wave Climate*.

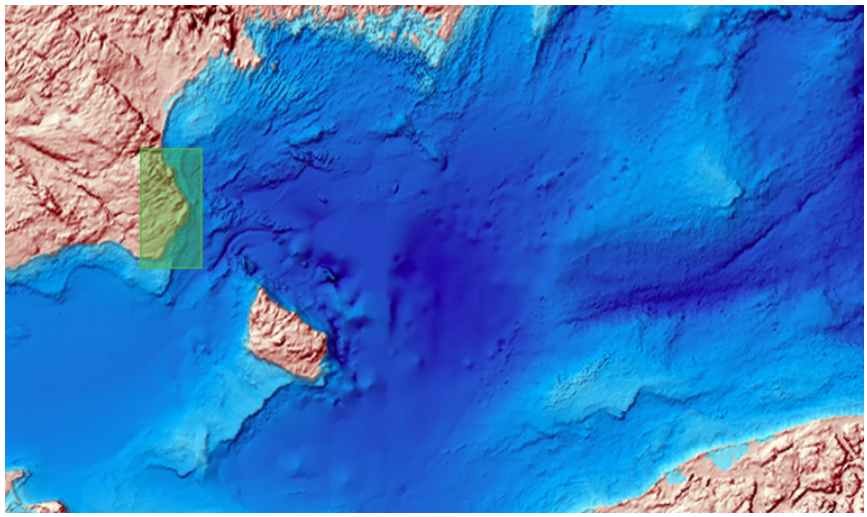

Figure 6: The offshore bathymetry of the Baltic Sea. Image: Baltic Sea Hydrographic Commission, 2013, Baltic Sea Bathymetry Database version 0.9.3. Downloaded from http://data.bshc.pro/ on May 25, 2016.

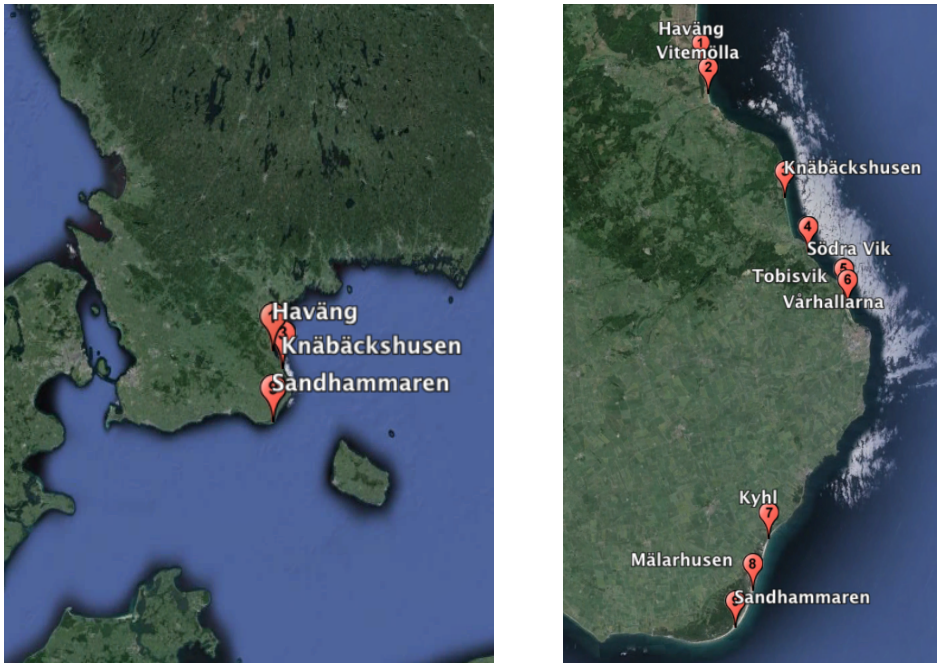

(a) Scania (b) Southeastern Scania

Figure 7: Study area. Graphics: Google Earth 2016

The beaches were visually examined on 3rd of March 2016 and a great diversity in beach morphology was evident. The beaches range from wide, flat beaches with fine sediments to steep, partly embayed beaches with coarser sediments. When looking at historical photos of the beaches, it is obvious that some areas are very dynamic. Knäbäckshusen is one especially dynamic area, as can be seen in Figure 8.

(a) 2005 (b) 2006

Figure 8: Morphological change of Knäbäckshusen between 2005 and 2006. Photo: (a) Linköpings Häng och Skärmflygsklubb, (b) Mattias Regnell.

3.2 Bathymetry

The bathymetry of the Coast of Scania was surveyed by the Geological Survey of Sweden (SGU) from 2012 and throughout 2014. Hydroacoustic measurements were performed by SGU vessels S/V Ocean Surveyor and S/V Ugglan to a depth of 2-3m. The shallowest waters were scanned by light detection and ranging (LIDAR) from an aircraft. High resolution bathymetry (1x1 m raster) of some areas are under military secrecy and can only be viewed at SGUs head office in Uppsala. However, bathymetry with lower resolution (2x2 m raster) are available for research purposes. The confidential data was studied on March 11, 2016 to obtain an overview of the beach morphology of the coast. The coast of interest show a wide variety and range from fully dissipative to reflective beaches with several intermediate stages present. Below follows a visual analysis of the bathymetry. Unfortunately the bathymetry for the three southernmost beaches are under complete military secrecy. The analysis also includes findings from the field visit on March 4.

The beach in Haväng (Figure 9) show clear signs of cresentric bars closely attached to the beach face, but also tendencies of deeper isolated pools. One or more of the pools also seem to have narrow, shore-perpendicular channels. The irregular shape of the coastline in the southern part probably arises from the presence of partially submerged large rocks. The beach face have small, regular beach cusps with a wavelength of 4 - 5m.

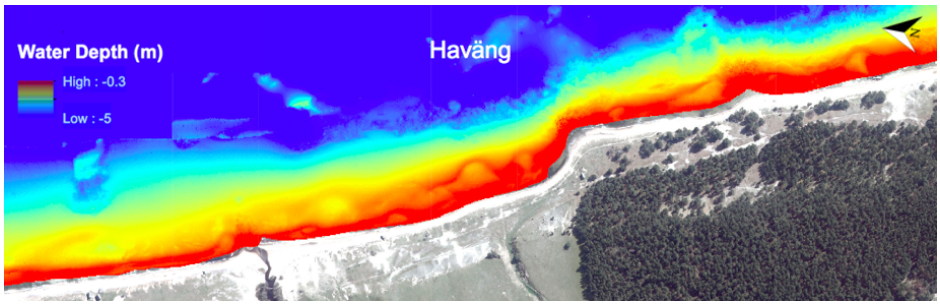

Figure 9: Haväng Beach with cresentric bars and signs of isolated pools. Background image: GSD-Ortofoto, 1m färg © Lantmäteriet I2014/00579. Bathymetry: 2m © SGU.

The beach north of Vitemölla harbor (Figure 10) seems to have an even more accentuated cresentric bar shape. In contrast to Haväng the bars also have a skewed appearance. Furthermore, the bars outside some deeper pools seem not to be especially accentuated. The beach have cusp-like formations with a wavelength of 150 - 200 m which partly could be explained by submerged rocks 50 m from shore acting as sediment traps.

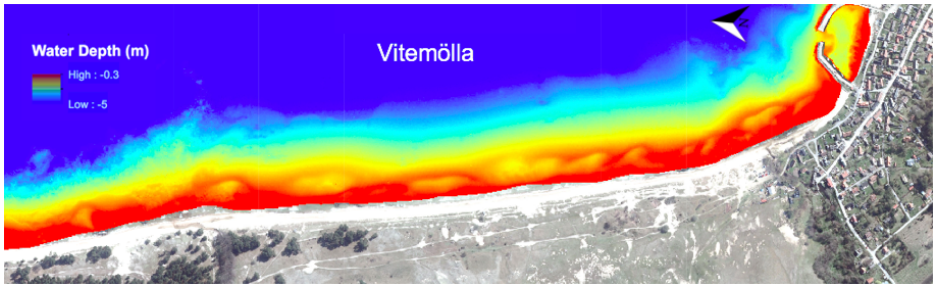

Figure 10: Vitemölla beach with large longshore bar variability with cresentric tendencies. Background image: GSD-Ortofoto, 1m färg © Lantmäteriet I2014/00579. Bathymetry: 2m © SGU.

The bathymetry of Knäbäckshusen (Figure 11) show long shore-parallel bars without any major indications of irregularities or current channels. The outer bar is very large and have a mild rhythmic shape. In the southern part it shows a tendency to extend landward. As a whole, the shapes and extensions of the bars somewhat resemble a intermediate/dissipative beach in the Beach State

Classification by Wright and Short (1984). The beach has an irregular width and small patches of the beach is covered with larger stones.

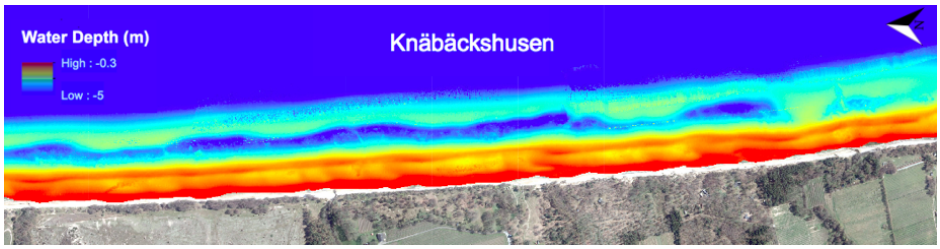

Figure 11: Knäbäckshusen with several parallel well developed bars. Background image: GSD-Ortofoto, 1m färg © Lantmäteriet I2014/00579. Bathymetry: 2m © SGU.

Vårhallarna (Figure 12) is a pocket beach enclosed by two cliffs. There are no signs of any bars and the beach slope is steep, resembling a reflective beach. The foreshore also contains large rocks.

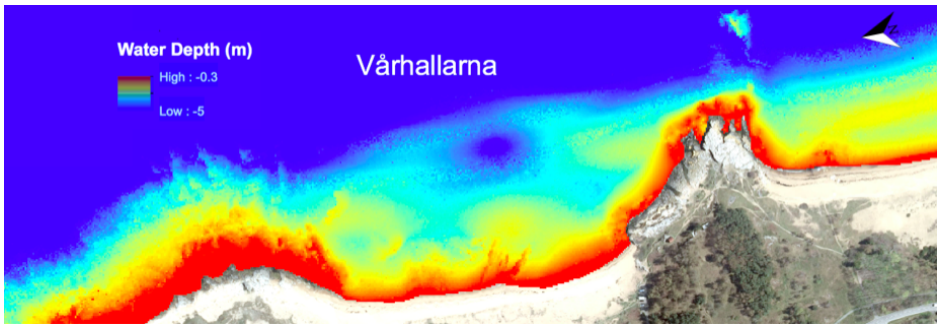

Figure 12: Vårhallarna with a steep foreshore and no signs of bars. Background image: GSD-Ortofoto, 1m färg © Lantmäteriet I2014/00579. Bathymetry: 2m ©.

Just south of Vårhallarna, Tobisvik Beach stretches to the harbor of Simrishamn. The beach slope is very steep and vague, cresentric and wide bars can be seen. In some parts of the beach the bars seem to have attached to the beach face.

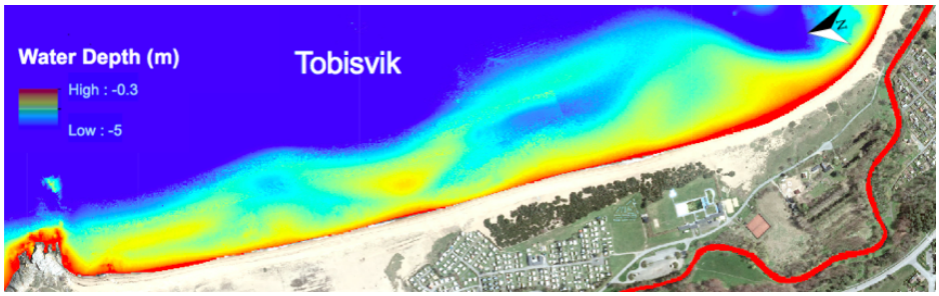

Figure 13: Tobisvik showing a steep foreshore and weakly developed bars. Background image: GSD-Ortofoto, 1m färg © Lantmäteriet I2014/00579. Bathymetry: 2m © SGU.

3.3 Wind and Wave Climate

The Baltic Sea has a limited fetch thus no long period swells exists. The wave climate is dominated by short period wind waves and the waves are almost always accompanied by strong onshore winds. Even though wave action is the largest driving force, wind stresses have been shown to have considerable influence on nearshore currents (Hubertz, 1986). This chapter aims to give an overview of the wind and wave climate within the study area. Wind data, collected from SMHI Open Database is graphically presented and is also used as input to a wave model. All data and model output are presented in frequency roses. Frequency roses visualizes the frequency of both wind speed/wave height and the direction of these. The length of the vector in each direction represent the direction frequency while the colors represent the wind speed/wave height frequency.

3.3.1 Wind Climate

Wind data was collected from from three stations; Simrishamn (1951-1966), Sandhammaren (1966-1995) and Skillinge (1995-2015). The stations hourly register wind speed and direction and all stations are within the study area. By visualizing the data in wind roses (Figure 14), an overview of the wind conditions are attained.

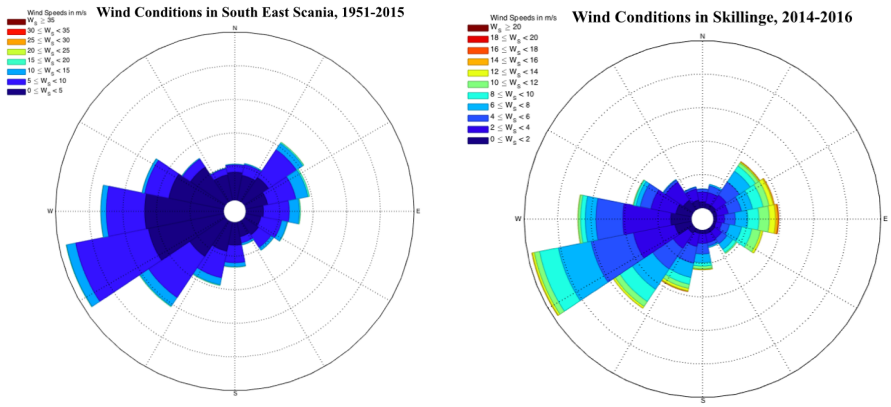

(a) 1951-2015

(b) Jan 2014 to March 2016

Figure 14: Wind direction and speed for the study area. Note that the scale for the two figures differ.

From Figure 14a it can be seen that the dominant wind direction on the longer time scale (1951-2015) is from west and southwest. It is also evident that the easterly winds more often reach speeds above 10 m/s compared to wind from other directions. The wind data from the early years unfortunately have gaps in the data (every hour is not in the data set) and therefore the wind from the later years is overrepresented in Figure 14a. As the wind climate over the Baltic Sea determines the wave climate, the wind observations from 2014 and to present date are data of interest (Figure 14b). The wind climate during these years is the main parameter determining how the bathymetry has changed since it was measured. Also during these years, the prevailing wind direction is from west-southwest but it is further evident that the coast has been object to strong winds with speeds above 20 m/s. These storms have definitely had a great impact on the sediment transport on the beaches within the study area.

3.3.2 Wave Climate

To evaluate how the wave climate varies along the coast, a wave hindcast simulation for the last 20 years (1996-2016) was performed. The wave hindcasting is based on the methodology described in U.S. Army Corps of Engineers (1984), which is commonly referred to as the SPM-method (Shore Protection Manual). The set of equations allow calculation of deep water wave height with input parameters being fetch, water depth, wind speed and duration of wind. A com-

plication with using this method is that it requires a constant wind speed as input while the data set from actual wind measurements is continuously varying. To handle this wave growth and decay, the additional memory function by Hanson and Larson (2008) was utilized. The theory is explained in *Appendix* under chapter *SPM-MF*.

Four locations; Vitemölla, Knäbäckshusen, Tobisvik and Sandhammaren (see Figure 15) were chosen and using EMODnet (European Marine Observation and Data Network) fetches and average depths for all locations was collected.

Figure 15: Locations chosen for wave climate modeling: 1) Vitemölla, 2) Knäbäckshusen, 3) Tobisvik, 4) Sandhammaren. The locations for the wind stations Hanö and Skilling are also included. Graphics: Google Earth 2016

The fetch was extracted with a angular resolution of 10° which thereafter was interpolated to attain the full fetch spectrum. The wind data was collected from SMHI Open Database as in previous chapter (Skillinge 1996-2016). The wind speed resolution was 0.1 m/s and angular resolution 1°. Deep water wave heights were thereafter hindcasted with the SPM-MF methodology. It is important to remember that the model calculates wave heights based on the geographical fetch, which is a rather coarse assumption since the wind fields often are not uniform or do not stretch along the entire fetch. The data from Skillinge was compared with data from a SMHI station at Hanö. It was found that wind speed observations from the latter station was significantly higher (see Figure 43 and 44 in Appendix A). The wind recordings from Skillinge was though assumed to be most relevant

as input data since it is in the center of the study area. The result from the model is presented in Figure 16 - 17.

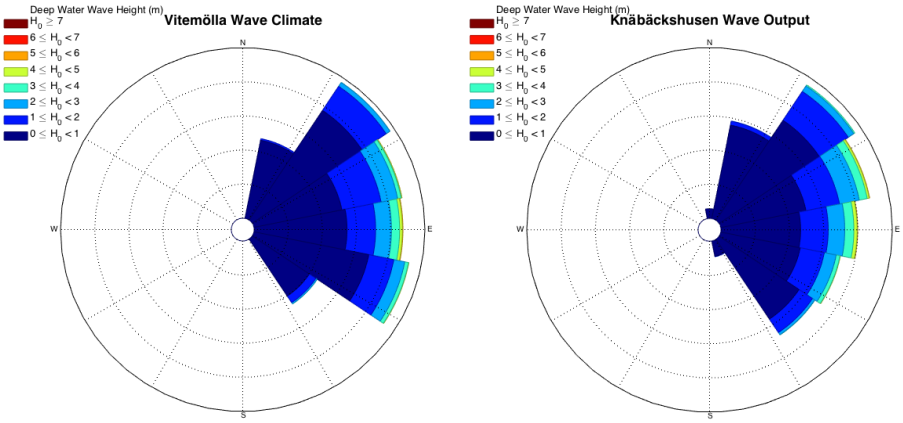

(a) Vitemölla wave climate (b) Knäbäckshusen wave climate

Figure 16: Deep water wave height and direction for Vitemölla and Knäbäckshusen.

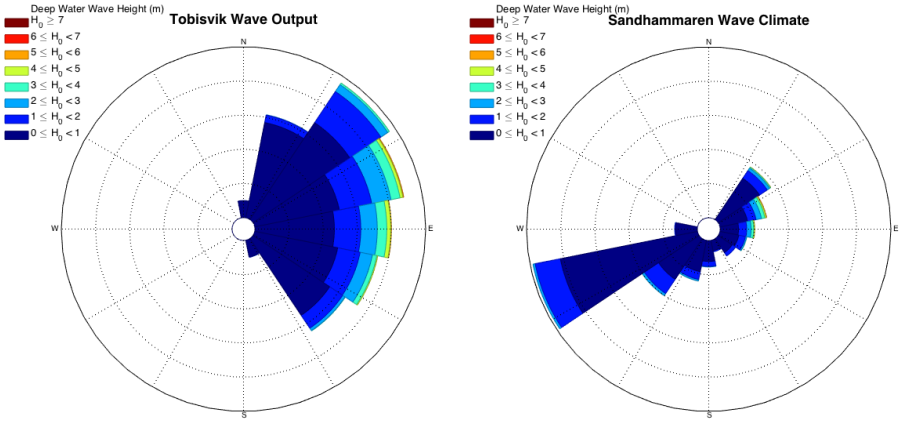

(a) Tobisvik wave climate (b) Sandhammaren wave climate

Figure 17: Deep water wave height and direction for Tobisvik and Sandhammaren.

The frequency roses implies that the beaches on the east coast have a very similar wave climate. Vitemölla though seem to be somewhat more sheltered from waves with a south component than the other beaches. Unlike the other beaches, Sandhammaren is very exposed to the frequent waves from southwest. Although, the wave height from this direction is rather low in comparison to the waves originating from the east. It is also evident that the island of Bornholm has a wave-shadowing effect for Sandhammaren.

3.4 History of Accidents

To investigate if there are certain beaches or weather conditions that are prone to increase swimming harzards, data over current-related drowning incidents was compiled from yearbooks of the Swedish Sea Rescue Society (SSRS). SSRS have had rescue stations at Kåseberga, Skillinge, Simrishamn, Kivik and Yngsjö and important events from every year has been included in the national yearbook. The wind conditions during the incidents were collected from wind station Skillinge and Hanö (depending on incident location). The data is presented in Table 1.

Table 1: History of accidents compiled from SSRS yearbooks. W_{dir} is wind direction in degrees north, W_{spd} is wind speed in m/s.

Date	**Location**	**Comment**	W_{dir}	W_{spd}
2015-07-17	Haväng	Two drowned in probable rip currents	80	10
2007-06-26	Löderup	Swimmer lost - made it back	180	5
2007-07-09	Ystad yttre vågbrytare	Problems getting up to pier	230	6
2006-07-20	Vitemölla	Air-matress drifted offshore - made it back	90	4
2005-08-15	Yngsjö Havsbad	Swimmer missing - not found	180	3
2004-07-04	Sandhamaren	Canoeists drifted 1000m	230	9
2003-08-05	Vitemölla	Swimmer found dead	300	3
2003-09-05	Vitemölla	Swimmer had problems getting up - made it	0	0
2002-08-11	Åhus	Swimmer missing - clothes on beach	90	7
1995-07-26	Åhus	Swimmer had problems getting up - made it	90	4
1995-07-31	Sandhammaren	Two caught in westward current - got up	70	6
1993-07-08	Rigeleje Okeröd	Two caught in current - drifted 500m	250	8
1993-07-28	Sandhammaren	Two caught in eastward current- one drowned	300	20
1984-08-27	Sandhammaren	Windsurfer in problem, longshore current	200	4
1979-08-08	Löderup	Windsurfer in problem, longshore current	90	6

3.5 Interviews with Local Fishermen

The incidents reported in SSRS's material is only a selection of rescue missions in the region and it is probable that there are many unrecorded events. To get greater understanding of the local currents and related accidents, two local

eel-fishermen were interviewed on October 14. Both fishermen agreed on that regular rip currents occur along the northern beaches when the wind is from NE-SE. Before the small harbors were built in respective area, local fishermen utilized the rip channels to avoid running aground. One fisherman based in Vitemölla claimed the rip currents to be stationary in contrast to the fisherman north of Haväng, where the rip channels seem to constantly move. When it comes to safety, both fishermen were raised to not enter the water as there were waves and they both request "red-flagging" during these conditions.

4 Drifter Development

The morphology of beaches can tell a lot about what currents are expected at different sites but in order to verify the theory, field measurements are desirable. There are several instruments available to measure currents and in general the measurements are divided into two main categories; Eulerian and Lagrangian. Eulerian measurements refers to observing the velocity of the water at a fixed place in space. As currents rarely are stationary but change with the beach morphology, Eulerian measurements will not give an overview of the large current system without installing multiple instruments. Lagrangian measurements on the other hand simply follows the track of a water parcel and thereby also gives information about the spatial behavior of the current. A frequently used method along ocean current researchers is deployment of so called drifters, a GPS-tracked floating buoy. Several attempts to build low-cost drifters have been made and with inspiration from these studies, drifters were designed and constructed to carry out field measurements.

4.1 Drifter Design

The proposed drifter design has similarities to PVC-drifters developed by Schmidt et al. (2003) but also with inspiration from Sabet and Barani (2011). The drifter design consists of 4 elemental parts: 1) a circular damper disc, 2) a pipe containing the GPS-device, 3) four vertical walls, 4) a flag rod. The outline of the drifter is presented in Figure 18.

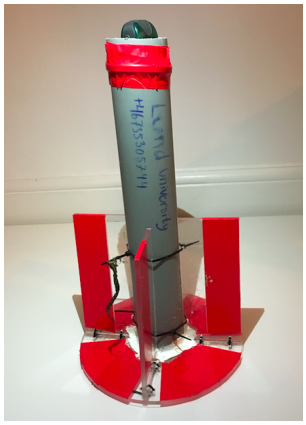

Figure 18: Constructed drifter, without the plastic sealing cover.

To prevent the drifter from surfing towards shore when exposed to breaking or near-breaking waves, the drifter was equipped with a damper disk with a diameter of 25cm. This dampens the vertical motion of the drifter and thus allows the drifter to pass over waves. To reduce the direct wind forcing on the body of the drifter, the drifter is nearly completely submerged by buoyancy weights attached close to the bottom of the drifter. These weights also help to reduce the deviation from an upright positioning that can disturb the GPS-performance. The four vertical walls provide sufficient area for the current to carry the buoy.

The dimensions of the drifter are similar to Sabet and Barani (2011) but finally determined by the dimensions of available commercial plumbing pipes ($d = 75mm$). The small size enables the equipment to be retrieved outside the breaker zone with a surf craft. The GPS-devices (Garmin eTrex Venture) are of non-differential type with a spatial resolution of 15m and a maximum sampling frequency of 1Hz. The data in the experiment by Sabet and Barani (2011) was collected with similar equipment.

4.2 Drifter Construction

The damper disc and vertical walls were cut out from 5 mm thick acrylic plastic using a CNC router. The center pipe was cut out from commercial plumbing pipes (d = 75mm) and the drifter was assembled with two component epoxy glue and cable ties. To assure that the center pipe is waterproof, the seams were sealed with acrylic sealant on the outside and silicone on the inside. To attain enough buoyancy and stability, the lower section of the pipe was filled with approximately 450 g of iron nails and polyurethane foam. Room for the GPS was cut out from the foam and the top of the drifter was covered by thick construction plastic sealed by cable ties.

4.3 Drifter Velocity Calculations

The drifter position was continuously registered by the GPS-units at a 5 second interval. To calculate the velocities, the data was converted into a metric coordinate system (SWEREF99 TM) using *Deltares Open Earth Tools*. When the drifter submerges as a wave pass over it, the GPS accuracy could temporally decrease. Large deviations between two sampling points would result in overestimated current velocities. To cope with this, data with such tendencies was filtered with a zero-phase filter (moving average) in both backward and forward direction (20s). This process causes each data point to obtain the average position of the four nearest neighbors. The distance between data points could be calculated through Pythagoras theorem and the velocity could thereafter be

found simply by dividing the distance by the sampling time (Equation 17).

$$v = \frac{\sqrt{X_{avg}^2 + Y_{avg}^2}}{t} \ (m/s) \tag{17}$$

Where X_{avg} and Y_{avg} are the distances between adjacent filtered coordinates and t is the time interval (5 s). To evaluate the filter performance, the processed velocities were plotted against velocities calculated from raw data, see Figure 19 for an example.

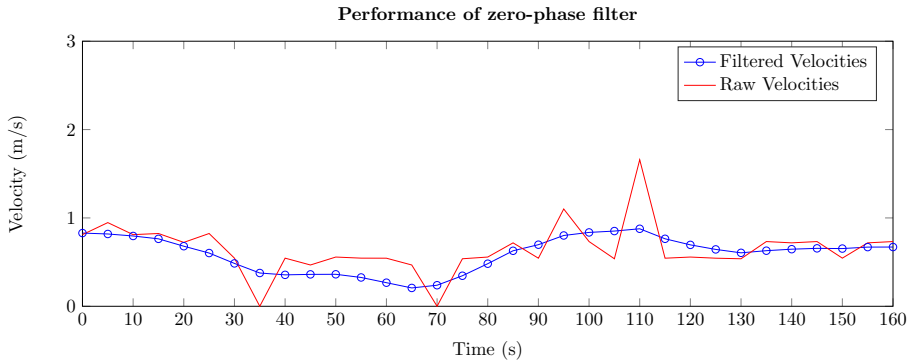

Figure 19: Velocities from processed data in comparison to velocities calculated from raw data.

It is important to keep in mind that when filtering data, valuable information might be lost. For example, shore-perpendicular movements that occur on a short time scale would appear as less accentuated and the cross-shore velocities would turn out significantly lower. This can be seen in Figure 19 at Time 110 s. Evaluating the raw data before filtering is therefore of great importance. For example, a longshore current without any major signs of shore-perpendicular flows should to a larger extent be safe to filter whilst data with jagged offshore movements should be filtered with care. In the latter case it could be suitable to isolate the interesting episodes and avoid excessive filtering when calculating the velocities.

5 Field Measurements

MacMahan et al. (2006) stated that complete in-field experiments of rip currents requires three types of measurements:

1. Velocity measurements in both the rip channel and across the breaker.
2. Bathymetry measurements with good resolution.
3. Measurements of offshore directed waves (infragravity waves).

Measurements of offshore directed waves are technically advanced since it requires several wave pressure gauges (or wave buoys) and furthermore thorough frequency analysis to find the spectrum representing infragravity waves. The theories behind how infragravity waves interact with incident waves and the morphology is still under discussion amongst researchers and this thesis therefore exclude these measurements.

5.1 Complementary Bathymetry Measurements

To evaluate how the morphology of the beaches changes with time a bathymetric field measurement was performed on April 7. This measurement also aimed to increase the resolution of the bathymetry in the shallowest water. By the use of a RTK-GPS, the beach profiles from the back of the dune to a water depth of 1.6 m were measured by walking and sampling at representative points. The equipment used was a TOPCON GR-3 with 10 mm height accuracy.

5.2 Grain Size Sampling

Grain samples from respective beaches were collected on April 7 and was thereafter analysed by sieving. Narra et al. (2015) found that that the upper foreshore (at high tide) is the best place on the beach to sample to attain a sample that is representative as a median size of the beach profile. Thus, the sediment was collected at this point throughout the nine beaches. In the laboratory, a setup of sieves with different mesh sizes was assembled. The mesh size is presented in Table 2. The most commonly used parameter to describe sediment sizes is the mass-median-diameter, D_{50}. The D_{50} was thereafter calculated through a MatLab script of Fredriksson (2015).

Table 2: Sieve Setup

Mesh Size (mm)	2	1.4	0.71	0.5	0.355	0.25	0.18	0.125	0.09	0.063

5.3 Drifter Measurements

When the wind conditions were sufficient to generate waves, drifter measurements were initiated. Because of the limitations in time, only four measurements were undertaken. The drifters were released in the the surf zone and when the it was stranded or exited the surf zone, it was retrieved with a surf board. Measurements were done at:

- Sandhammaren, 7 April 2016
- Vitemölla, 26 April 2016
- Knäbäckshusen, 31 May 2016
- Vitemölla, 17-18 September 2016

6 Field Measurement Results

6.1 Grain Size Sampling

The result from the grain size sampling is presented in Table 3 and Figure 20. The D_{50} is ranked in ascending order. Table 3 also includes $\frac{D_{84}}{D_{16}}$ which is a common parameter used when evaluating the grain size sorting. Lower ratios describe a narrower distribution of grain sizes in the sample.

Table 3: Grain Size properties of the nine beaches, D_{50} in mm.

	Sandhammaren	**Mälarhusen**	**Kyhl**	**Knäbäckshusen**	**Vitemölla**
D50	0.1879	0.2026	0.2146	0.2898	0.3080
D84/D16	1.468	1.461	1.476	1.482	1.494
	Haväng	**Södra Vik**	**Vårhallarna**	**Tobisvik**	
D50	0.3578	0.5385	0.6126	1.0258	
D84/D16	1.496	1.497	1.464	1.496	

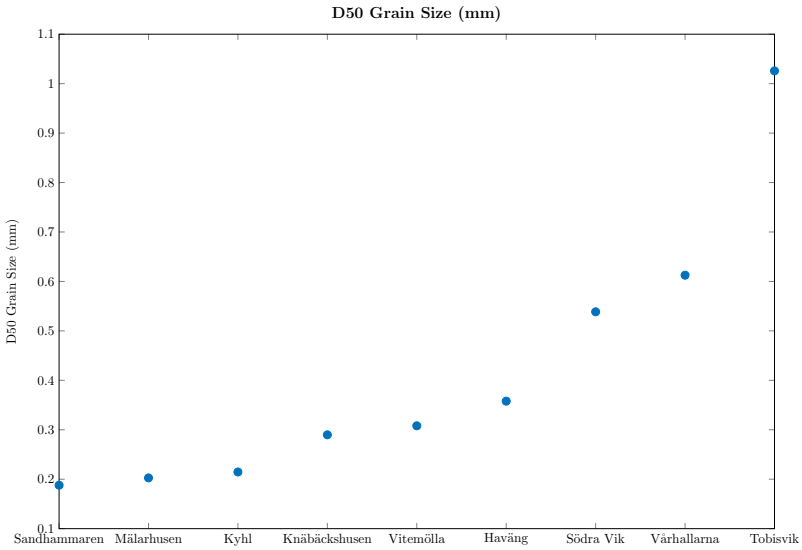

Figure 20: D_{50} grain size at the nine beaches in ascending order.

The result from the grain size sampling shows that the beaches of Sandhammaren, Mälarhusen and Kyhl all have very fine or fine sand. Tobisvik and Vårhallarna

have very coarse or coarse sand whilst the rest of the beaches have medium sand according to Wentworth size chart (Wentworth, 1922).

6.2 Complementary Bathymetry Measurements

The field data from April 7 was analyzed in ArcGIS and the profiles are presented in Figure 21 - 23. The profile elevation has been adjusted according to the mean sea level on basis the measurements by SMHI (2016). Included in these figures is also the data from the field measurements of SGU from 2012-2014. The data is extracted from the digital elevation model with 2x2 m resolution. It is evident that the beaches of Knäbäckshusen and Vitemölla have had a morphological change since 2014; the innermost bar seem to have migrated shorewards. Since the methodology only allowed measurements to 1,6 m depth, any conclusions about the steeply sloping beaches in Figure 22 can not be drawn (the overlap is just too short). Figure 23 shows that the three southernmost beaches have a dissipative beach state, as predicted by visual inspection and aerial photos. The large accumulating dunes at Sandhammaren and Mälarhusen are also evident in the same figure.

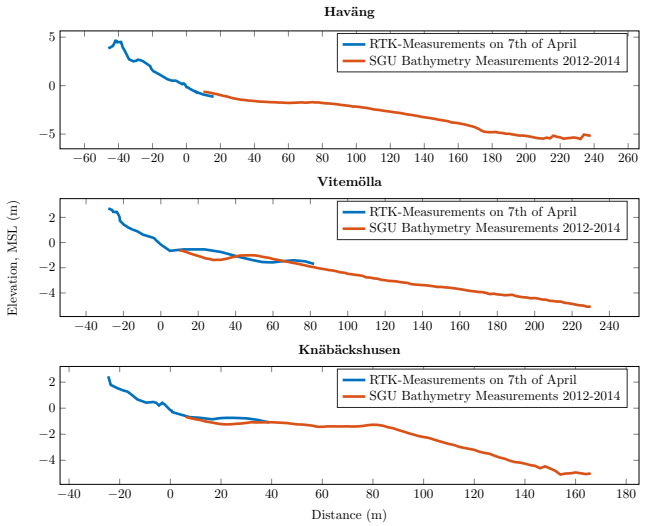

Figure 21: Measured beach profiles and comparison with SGU data.

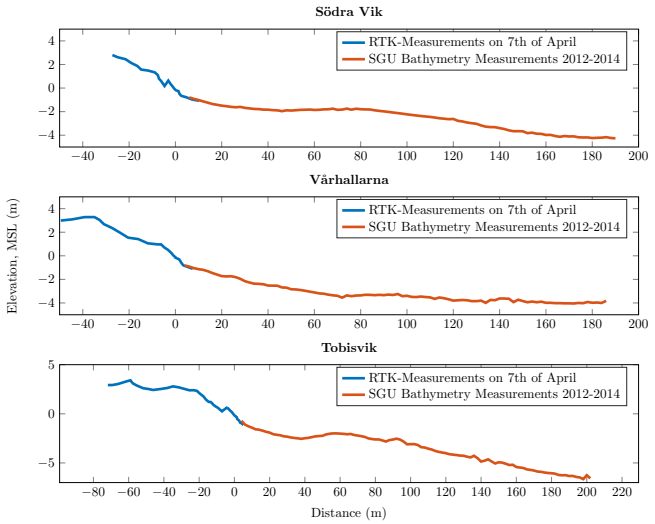

Figure 22: Measured beach profiles and comparison with SGU data.

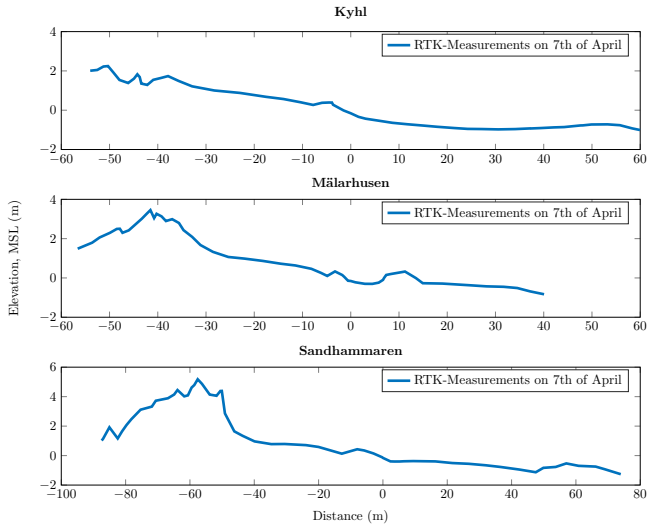

Figure 23: Measured beach profiles.

6.3 Summary of Beach Properties

Table 4: Properties of the nine beaches

Beach	Orien.	D_{50}	NS Slope	Beach State	SL Evolution
Sandhammaren	SE	0.188	0.012	1	+ 30-200m
Mälarhusen	E	0.203	0.014	1	+ 30-200m
Kyhl	E	0.214	0.012	1	+ 15-30m
Tobisvik	E	1.026	0.060	5 - 6	- 15-30m
Vårhallarna	E	0.613	0.043	6	0
S.Vik	E	0.540	0.020	4 - 5	0
Knäbäckshusen	E	0.290	0.024	3	- 15-30m
Vitemölla	E	0.308	0.023	4 - 5	0
Haväng	E	0.358	0.016	4 - 5	0

The first row shows the orientation of the shoreline (Orien.). The nearshore slopes (NS Slope) were chosen as the slope from shoreline to the 3m contour. The beach state was estimated from the resemblance with the state in illustrations by Wright and Short (1984). The modal beach state parameter Ω is not applicable since the coast of Scania most of the time do no receive any waves. Although, visual determination of the beach state can be of interest anyways since it partly determines the expected current patterns. The shoreline evolution between 1939-2012 (SL Evolution) was studied by Persson et al. (2014) based on aerial images.

6.4 Current Tracking with GPS-Drifters

This chapter presents the results from drifter experiments and discusses what types of currents that were observed at the different beaches.

6.4.1 Sandhammaren April 7

The first field measurement of nearshore currents was performed on April 7 at Sandhammaren Beach. The wind speed and direction is graphically presented in Figure 24. The average wind speed was 8.7 m/s with a prevailing direction of 230° which is almost parallell to the shoreline. The breaking wave height was visually determined to 1.0 - 1.5 m and the waves had an oblique attack.

The drifters were deployed seaward of both the first and second bar (approximately at 1.3 and 1.8 meters depth). As seen in Figure 25, a longshore current with speeds ranging from 0.2 to 1.3 m/s and mean velocity of 0.62 m/s was observed. Unfortunately the experiment had to be cancelled since the sealing cap

of the drifters was found not to be completely waterproof. The ideal measurement would be on a longer temporal and spatial scale, since possible rip currents theoretically could have a 1000 m spacing and also vary temporally.

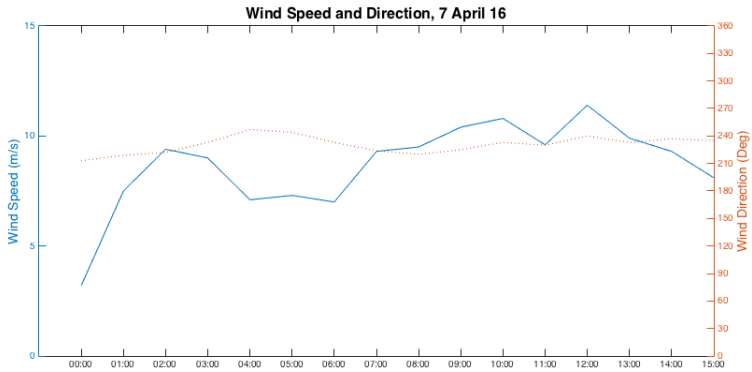

Figure 24: Wind speed and direction on 7th of April. The field work started at approximately 12.00.

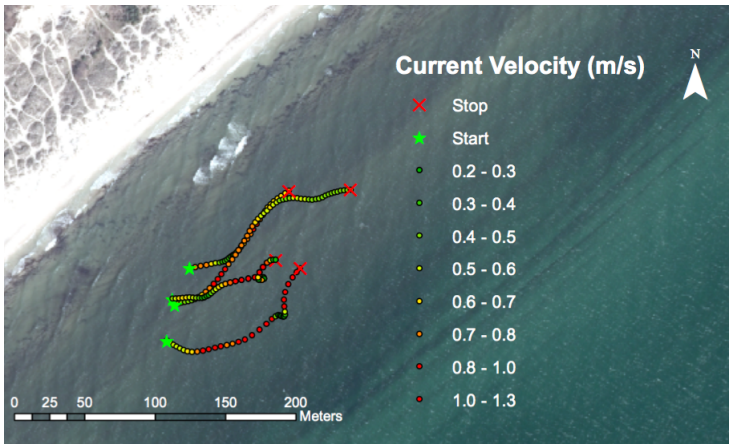

Figure 25: Results from the drifter experiment on April 7. Background image: GSD-Ortofoto, GSD-Ortofoto, 1m färg © Lantmäteriet I2014/00579.

6.4.2 Vitemölla April 26

The second drifter measurement was performed on April 26 at Vitemölla Beach. The wind speeds and directions are visually presented in Figure 26, the average wind speed was 9.7 m/s prevailing from southeast the hours before the experiment started. The breaking wave height was visually determined to 1.5-2 m with a slight angle from south, and it was also noted that the waves close to shore broke steeply, almost plunging. The drifters were deployed approximately 20-30 m from shore and instantly started drifting northward. Also this experiment suffered from problems as the drifters showed to surf shoreward with the steep waves. The drifters followed the shoreline at a distance of approximately 20 m from shore but it was clearly noted that the drifters encountered offshore directed flows on a regular distance of 100-150 m. These currents were very narrow and carried the drifters out to a distance of about 30-60 m from shore. Unfortunately the satellite connection was temporarily lost during some episodes when the drifters were carried shoreward by waves. The performance of the drifters and the increasing wave height caused the experiment to terminate earlier than intended.

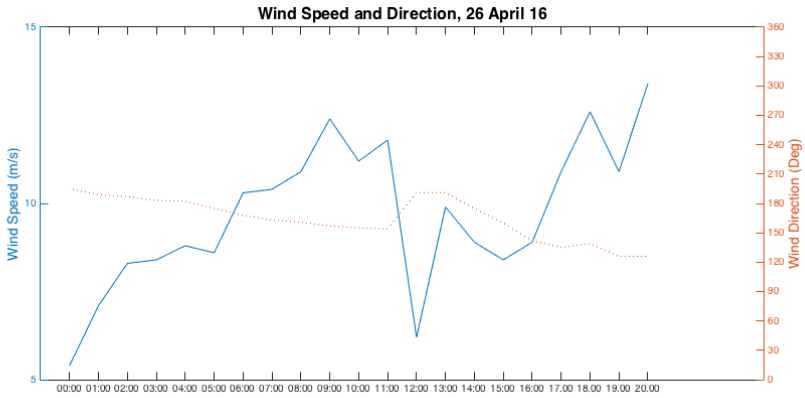

Figure 26: Wind speed and direction on 26th of April. The field work started at approximately 14.00.

One of the drifter tracks is presented in Figure 27 with velocities calculated for one isolated event. The grey points are the raw data, and the figure is slightly misleading since the drifter track is on the beach. This is probably due to deviations in the GPS-sampling. It is also obvious from the graphics that the data sampling was disturbed at times. If the full data series would have been filtered the offshore flow would definitely appear less accentuated and therefore only the

isolated event was filtered.

No surf zone exits or enclosed circulation cells were observed, it rather seems like a longshore current is meandering northward. Although, the movement of the drifters resembles a transient rip current under oblique waves as presented by Dalrymple et al. (2011) in Figure 4f. The clear meandering pattern of the longshore current differs from the measurements on Sandhammaren and this is likely due to the cresentric bar shape of Vitemölla Beach.

The velocity components are presented in Figure 28 together with the total velocity. The offshore-directed component is in the range 0.74 - 1.1 m/s which is significantly higher than observations in literature (0.2 - 0.7 m/s with storm peaks above 1 m/s (Shepard and Inman, 1950)).

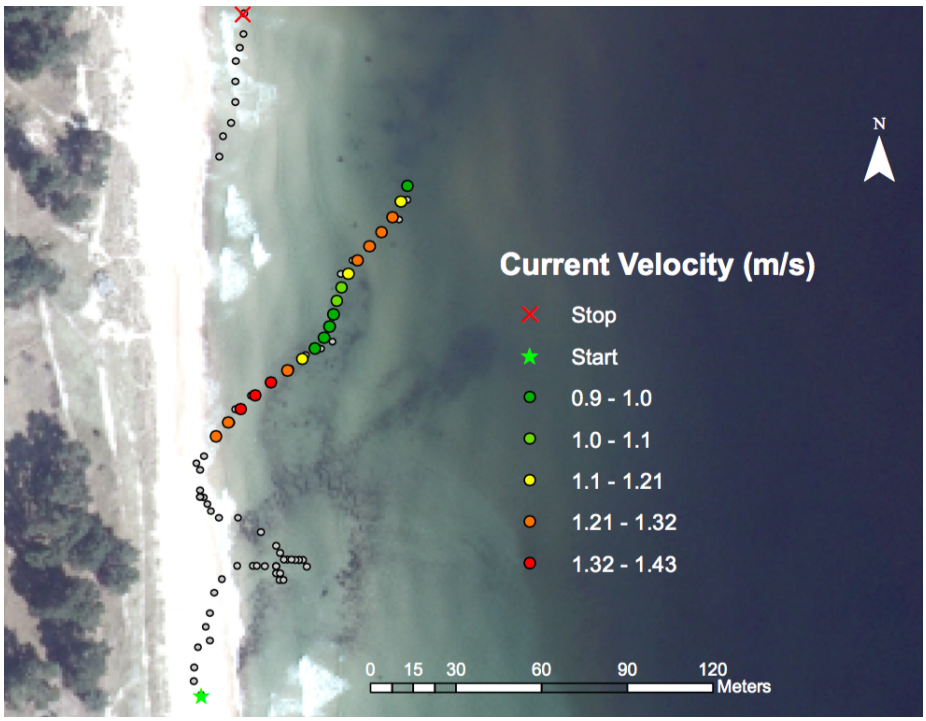

Figure 27: Results from the drifter experiment on April 26. Background image: GSD-Ortofoto, GSD-Ortofoto, 1m färg © Lantmäteriet I2014/00579.

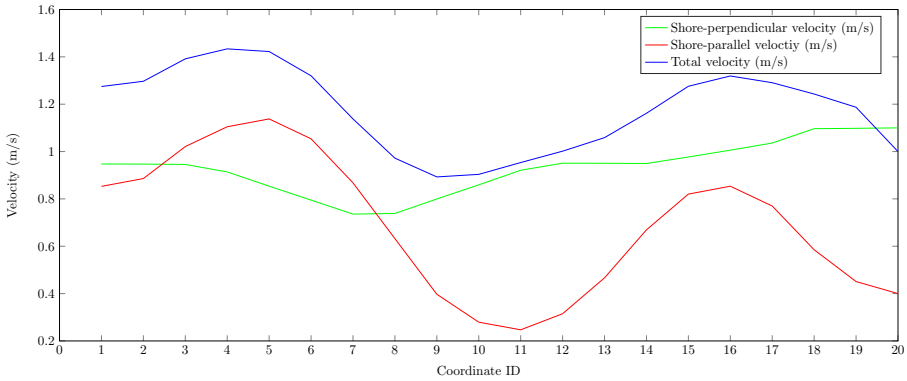

Figure 28: Velocity components for the drifter experiment on April 26

6.4.3 Knäbäckshusen May 31

On May 31 drifter measurements were performed at Knäbäckshusen. The north-eastern wind field over the Baltic did not extend all the way to shore and the wind at the beach was therefore very light (2 - 3 m/s). The breaking wave height was visually determined to 1 - 1.5 m with an oblique angle of about 30° from the beach normal. The data analysis shows a southward longshore current with a mean velocity of 0.39 m/s. The drifters mostly moved within the trough inside the first bar and therefore show a meandering motion, see Figure 29.

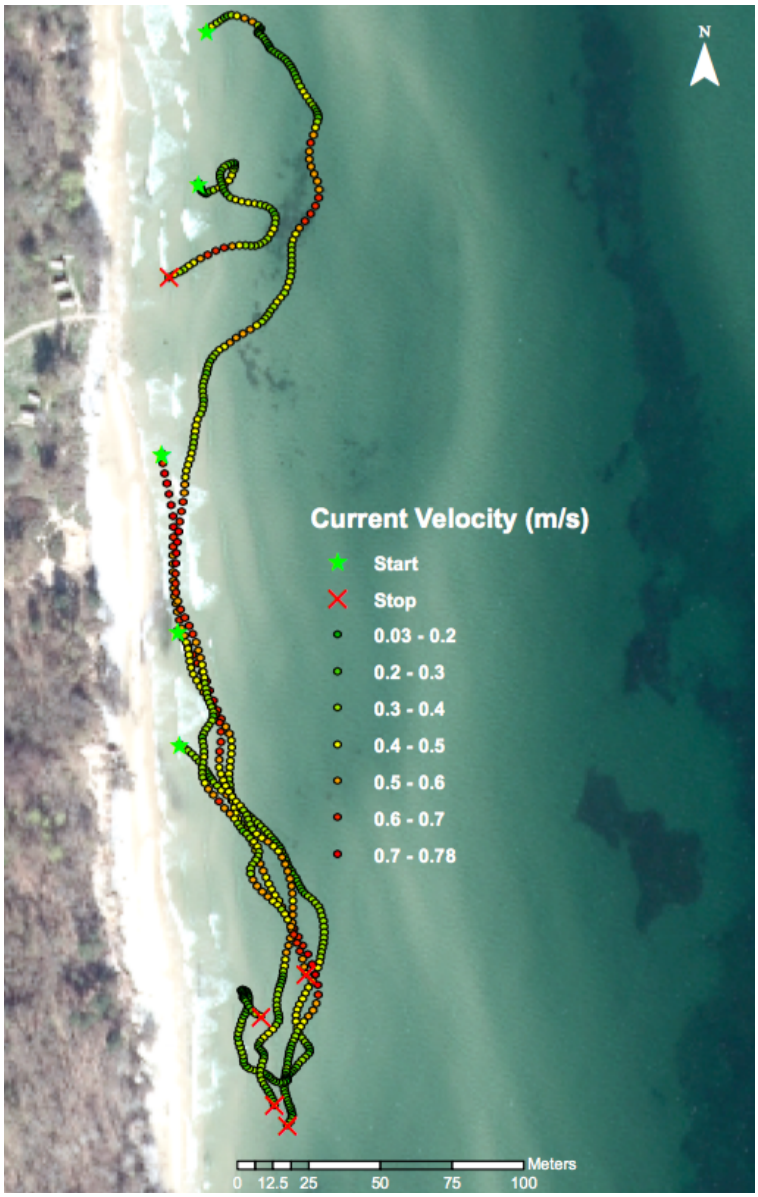

Figure 29: Results from the drifter experiment on May 31. Background image: GSD-Ortofoto, 1m färg © Lantmäteriet I2014/00579.

6.4.4 Vitemölla September 17-18

On September 17 and 18, drifter measurements were performed in Vitemölla. The wind speed and direction was evaluated from two weather stations, both Skillinge and Hanö. It was concluded that the wind speeds from the latter station were the most reliable (10.4 m/s, 85°) in comparison with observed speeds. The wave height was visually determined to 1.8 - 2.2 m. The drifters were released at several different locations approximately 20 m from shore. Several individual circulation cells along the beach were discovered, as can be seen in Figure 30. The black lines symbolize the drifter tracks and the yellow arrows the main current directions. The most pronounced circulation cell (Cell 1, Figure 31) had offshore velocities of 0.40 - 1 m/s in a channel of approximately 15 m width. In most cases the drifter returned to the beach in a clockwise direction, but one drifter was also found to exit the surf zone and not return back towards the beach (Sep 17 - 19:31).

About 200 m north of this cell, two currents with different directions seemed to converge (feeder currents), but no offshore current was observed. The measurements are presented in Figure 32. Another 200m north of this area, a skewed circulation cell with a counter-clockwise circulation was found. The offshore current had an approximate angle of 45° from the beach and a slightly lower velocity than in Cell 1 (see Figure 33).

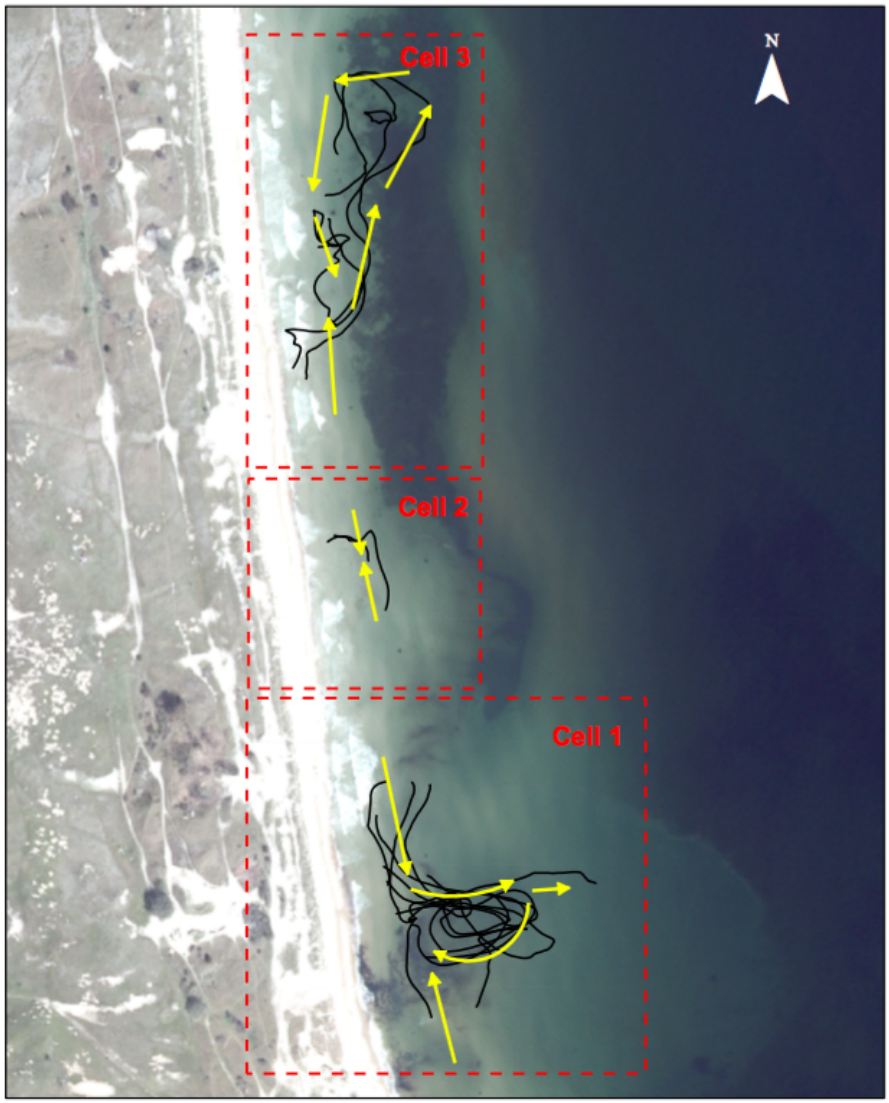

Figure 30: Results from the drifter experiment on September 17-18. Background image: GSD-Ortofoto, 1m färg © Lantmäteriet I2014/00579.

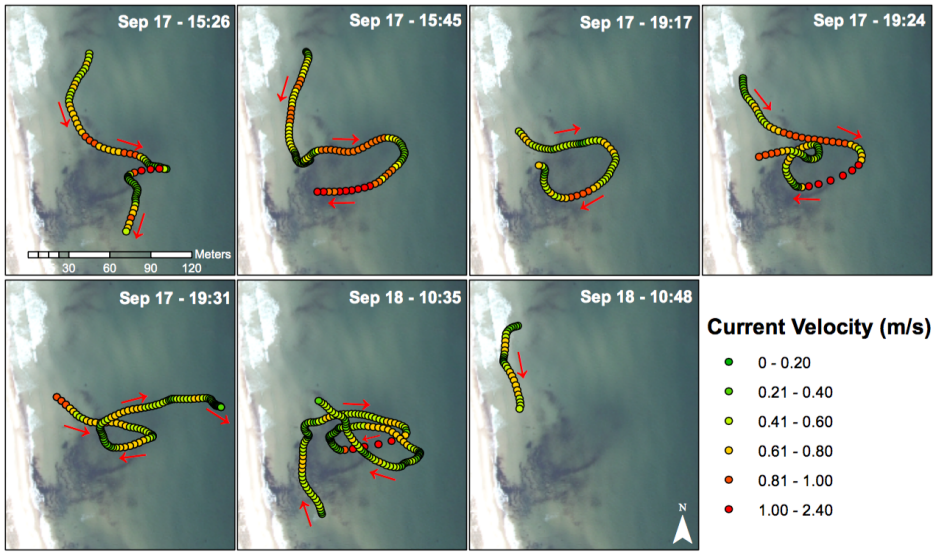

Figure 31: Results from the drifter experiment on September 17-18. Background image: GSD-Ortofoto, GSD-Ortofoto, 1m färg © Lantmäteriet I2014/00579.

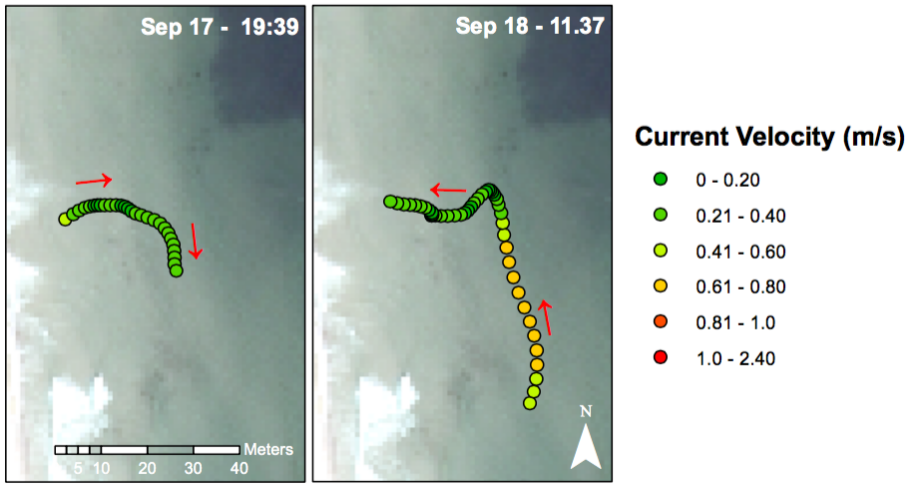

Figure 32: Results from the drifter experiment on September 17-18. Background image: GSD-Ortofoto, GSD-Ortofoto, 1m färg © Lantmäteriet I2014/00579.

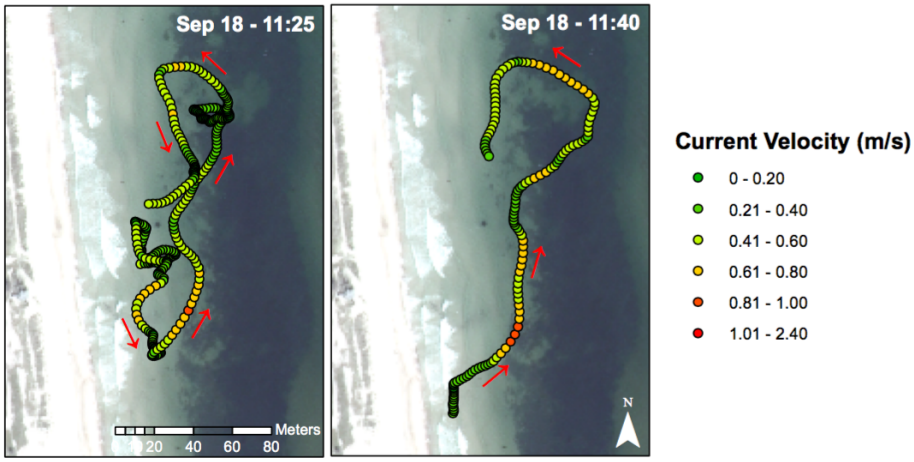

Figure 33: Results from the drifter experiment on September 17-18. Background image: GSD-Ortofoto, 1m färg © Lantmäteriet I2014/00579.

7 Numerical Modelling of Nearshore Wave Transformation

An approach to understanding the current systems is to model the wave conditions as the waves propagate onshore from deep water. In this study, this was done using the wave transformation model *EBED* developed by Mase (2001) and later modified by Nam et al. (2009). The physics behind the model is presented briefly under section *EBED* in *Appendix A*. The deep water conditions for respective field measurement were hindcasted using the SPM-MF and the output data is presented in Table 5. The conditions during the accident in Haväng 2015 was also calculated and are included in the same table.

Table 5: Wave conditions hindcasted with SPM-MF model for respective field measurement.

Location	**Date**	H_s	T_s	θ
Haväng	17 August 2015	4.1	8.2	96°
Sandhammaren	7 April 2016	0	0	N/A
Vitemölla	26 April 2016	1.5	5.6	60°
Knäbäckshusen	31 May 2016	0.2	2.2	90°
Vitemölla	17 September 2016	2.8	6.8	85°

Of the four field measurements, only the last measurement (17-18 September) was considered possible to investigate further using EBED. As the output from the SPM-MF model is used as input for the EBED model, the quality of this data is of great importance. Both for the measurements at Knäbäckshusen (May 31) and Sandhammaren (April 7), the SPM-MF underestimated the wave height (see Table 5). The wave decay of SPM-MF showed to be too rapid as the observed wave height during the field measurements at Knäbäckshusen was significantly larger than the hindcasted wave heights. Moreover, the SPM-MF model does not include diffraction and the waves hindcasted for the Sandhammaren event did not reach shore (the wind was almost parallel to the beach). The drifter data from the field measurements at Vitemölla (April 26) was finally considered to be of too poor quality to be valuable to compare with the EBED output.

7.1 EBED Simulation

The input data for the EBED model is bathymetry, offshore wave conditions and some computational parameters (such as grid size and spectral resolution). The bathymetry input in this case is an area north of Vitemölla harbour, streching approximately 1900m in the shore-parallel direction and 1000m offshore.

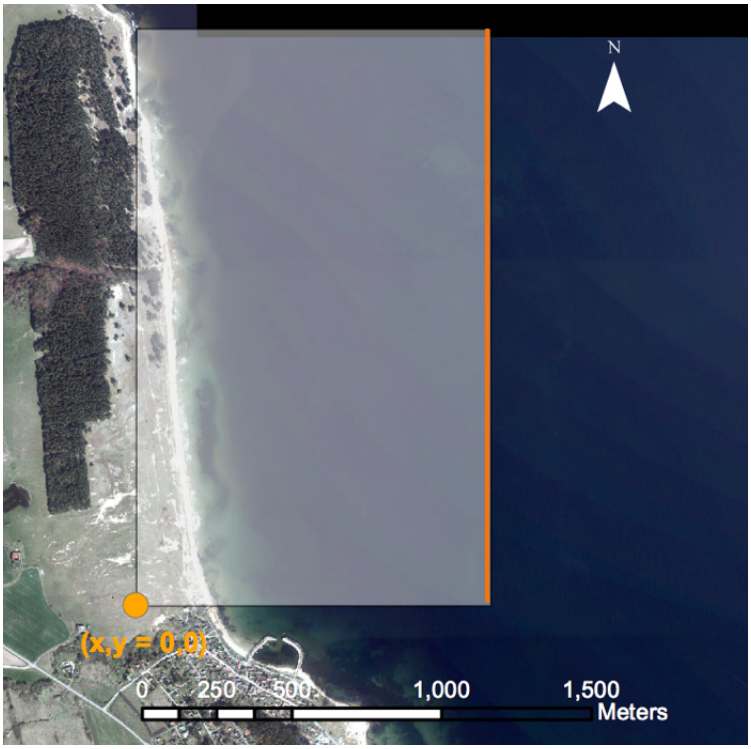

Figure 34: The extension of the bathymetric grid. The orange line represent the input boundary.

To reduce the run-time of the model, the bathymetry from SGU with 2 m resolution was transformed into a coarser grid with cell size of 5x5m. The offshore wave conditions (significant wave height H_s, significant wave period T_s, wave direction θ) were hindcasted with the previously described SPM-MF model. These wave conditions were set as boundary condition for the entire east facing grid (orange line in Figure 34). The model was applied for two events; the Haväng accident in 2015 and the event where a rip current was measured in September 2016. Both events were modelled with wave conditions hindcasted from both the Hanö and Skillinge wind station, see Table 6. Both events were modelled with the same bathymetry (even though the Haväng accident occured just north of this particular region).

Table 6: Wave Input for EBED model

Event	**Wind Station**	H_s	T_s	θ
Haväng	Hanö	4.1	8.2	96°
Haväng	Skillinge	1.2	5.7	65°
Vitemölla	Hanö	2.8	6.8	85°
Vitemölla	Skillinge	1.3	4.4	27°

7.2 EBED Simulation Results

The bathymetry of the grid area is shown in Figure 35. The point (x,y = 0,0) represents the SW-corner in Figure 34. It is evident that the north-east part of the grid has a shallow region where the bedrock reaches a depth of about 3m. The simulation in Figure 38 even indicate that the waves potentially can break over this elevated area.

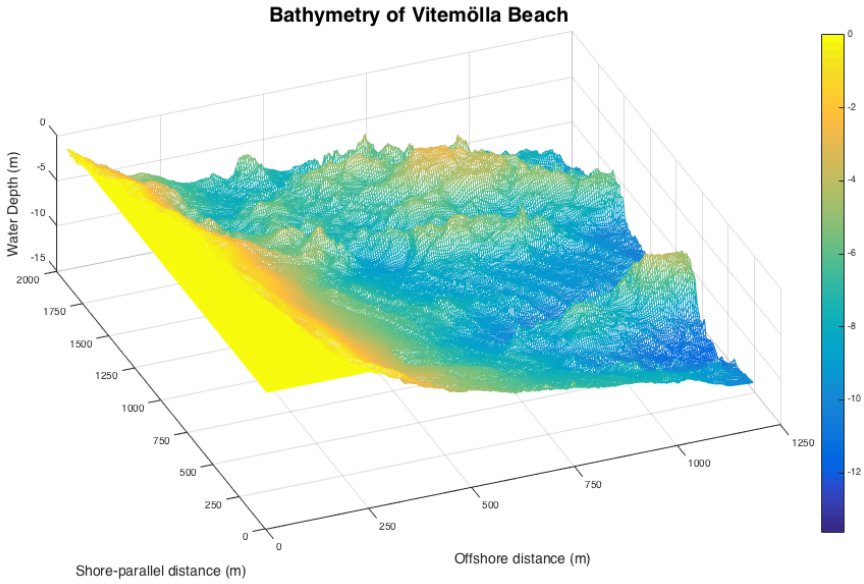

Figure 35: Bathymetry of the area of interest, just north of Vitemölla harbour.

7.2.1 Vitemölla - 17 September 2016 - 19:00

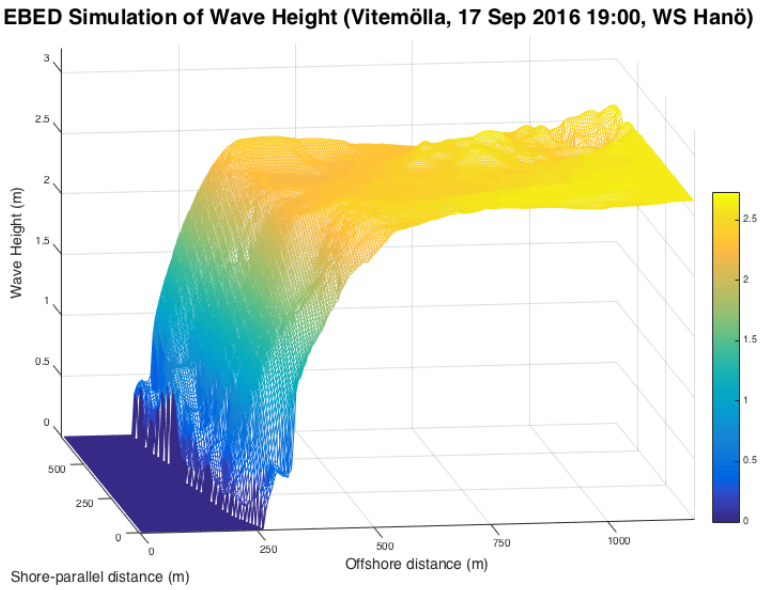

Figure 36: EBED-simulations with offshore wave conditions: $H_s = 2.8m$, $T_s = 6.8s$ *and* $\theta = 85°$.

Figure 36 displays that the model output indicates a longshore variation of wave height along the beach. This can be seen in the purple-blue area. A wave height variation of more than 0.5 m in only 100 m longshore distance implies that according to the model, there seems to be driving forces for nearshore currents on this stretch of beach. When comparing Figure 36 and 37 it is evident that the wave angle do not affect the nearshore variations in wave height significantly. Although, the 'overall' wave height is somewhat reduced by this oblique angle. The EBED simulation itself was found to be unable to predict the location of rip currents; the most accentuated rip current (Cell 1) from the drifter measurements was found at a distance of 160m from the SW-corner (y=160) as marked in Figure 36.

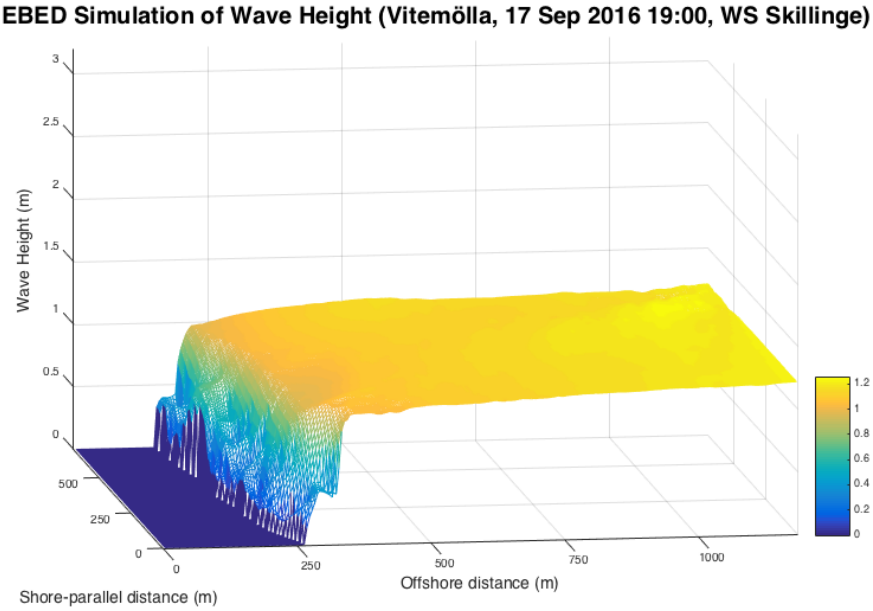

Figure 37: EBED-simulations with offshore wave conditions: $H_s = 1.3m$, $T_s = 4.4s$ *and* $\theta = 27°$.

7.2.2 Haväng - 17 August 2015 - 13:00

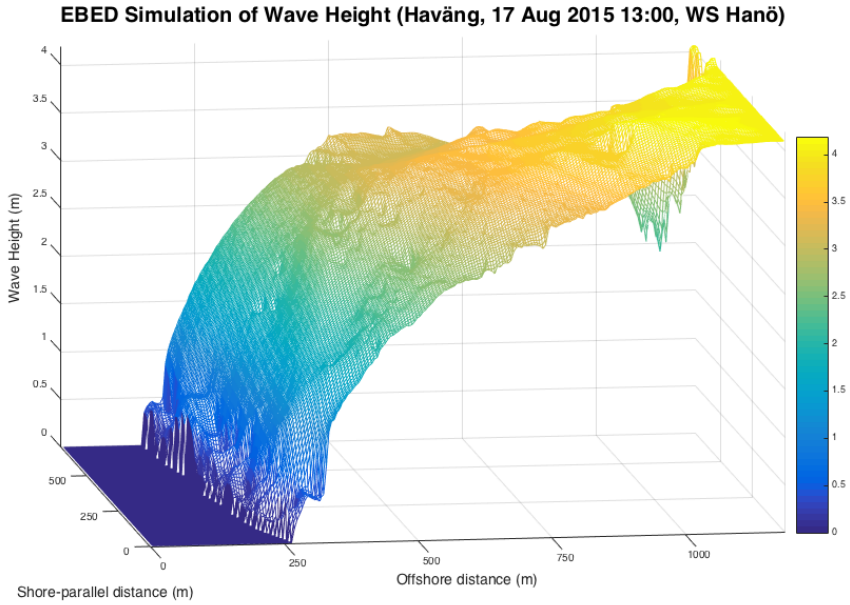

Figure 38: EBED-simulations with offshore wave conditions: $H_s = 4.1m$, $T_s = 8.2s$ *and* $\theta = 96°$.

It is clear that even though the wave height was significantly higher during the Haväng event, the nearshore variation in wave height is very similar to the field measurement event. However, the model displays that the surf zone is widened with increased wave height. Since the wave setup is related to incident wave height, it is possible to assume that both the offshore extension and speed of rip currents is larger for increased wave height.

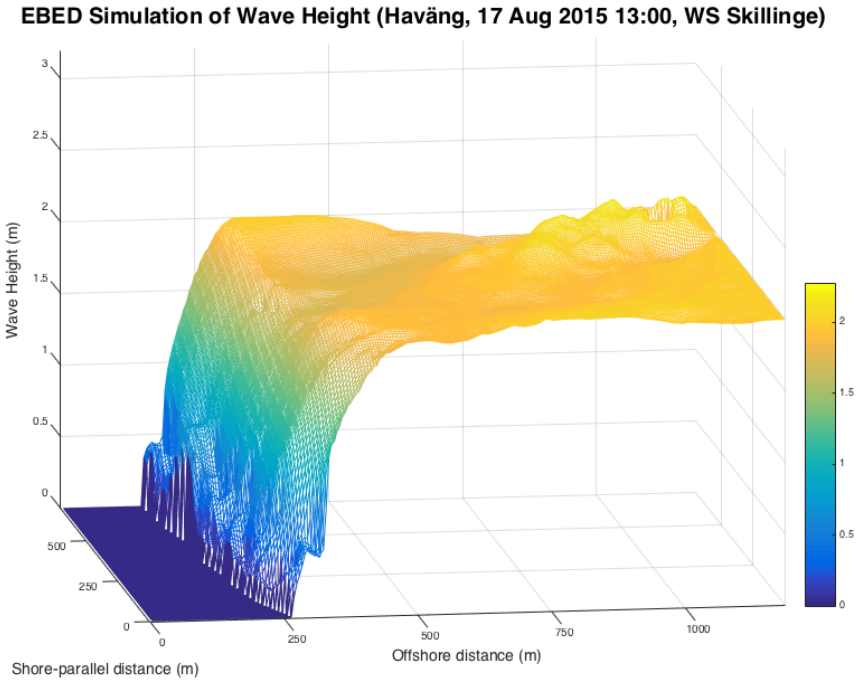

Figure 39: EBED-simulations with offshore wave conditions: $H_s = 1.2m$, $T_s = 5.7s$ *and* $\theta = 65°$.

One interesting finding is the fact that the wave height variation close to the shoreline is almost the same independent of offshore wave height. This is clarified in Figure 40. The lines represent the wave heights on a transect that follows the shoreline at a distance of 50m from shore. Even though the offshore wave height for the Haväng event is significantly larger, the wave height is only a couple of centimeters larger at the transect. Even if the wave height is not increased too much, it should be noted that the variation (between high and low waves) is increased for the high energy wave conditions. This could imply that the difference in wave setup would be larger in this case, and thus also the current driving forces.

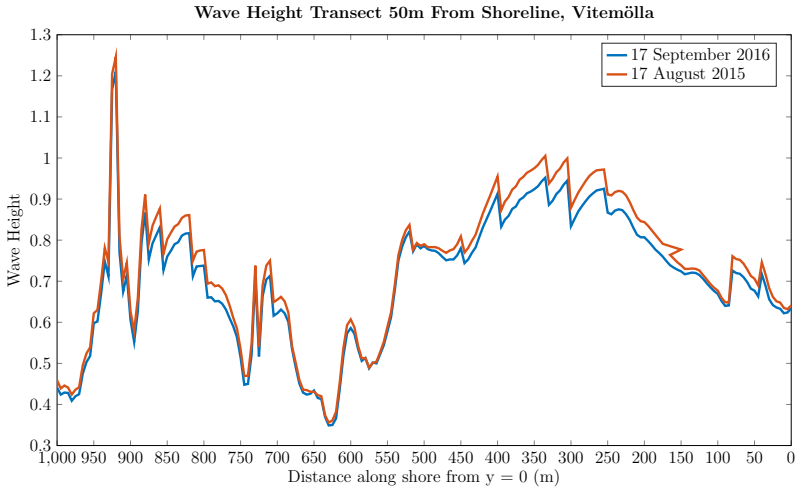

Figure 40: Longshore wave height variation 50 m from the beach.

7.3 Longshore Current Modelling

The longshore current for the Vitemölla accident was also modelled by the methodology of Longuet-Higgins (1971) described in the *Theoretical Background*. With the same data series hindcasted for the EBED simulations, the longshore current was calculated by Equation 13. In Figure 41, negative values velocities correspond to southward currents. The velocity during the first half of the measurements (Sep 17) was found to be very low (0-0.5 m/s) which might indicate rip currents. On the other hand, rip currents were also found the day after (Sep 18) when the modelled velocities reached above 1 m/s.

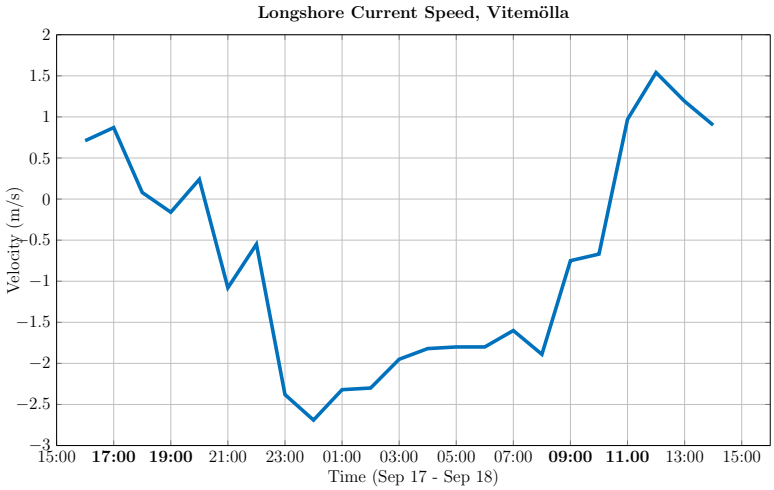

Figure 41: Simulation of longshore current on September 17-18 based on wave hindcasting and Longuet-Higgins methodology. The hours when the experiments were conducted are highlighted with bold font.

8 Discussion

The difference in morphology between the beaches within the study area was evident already after the first field visit on 3rd of March. The visit also raised several questions: Why are the beaches so different? Which beaches are stationary? Where can rip currents form? What are the hazards on each beach?

The following discussion is divided into five main parts:

1. **Drifter Experiment** evaluation: drifter design, GPS-accuracy and data analysis.
2. **Morphodynamics** analysis with respect to measured bathymetry and grain size.
3. **Data Analysis** and model evaluation.
4. **Safety Recommendations** for the municipalities and beachgoers, outline of a warning system
5. **Further Research** recommendations.

8.1 Drifter Experiments

The final design of the drifters proved to work very well in the modest wave conditions they were deployed in. The increased ballast weight and the deeper submergence of the fins gave better results; the drifters were less affected by near breaking and breaking waves and the satellite connection was greatly improved. The drifters are sufficiently robust and have good hydrodynamical properties for the purpose they were developed for, measuring currents in the nearshore region. Although, the fins could possibly be even smaller and maybe decreased to three in numbers to minimize the shoreward surfing even more. Some drifters in earlier studies have been equipped with drogues to reduce this surfing. In this study, drogues were found to impinge on the simple design and maneuverability. The GPS-accuracy was sufficient enough to establish an overview of the current systems (for example the three cells in Vitemölla) but in order to determine the velocities with high precision, a GPS base station on the beach would be desirable. Zero-phase filtering of the positions is somewhat a standard in drifter experiments but it has a significant influence on the velocities. A more accurate determination of the position would allow less filtering. However, it is not necessarily so that equipment with better spatial accuracy would yield better results for this study. Even though it might seem primitive to collect the drifters by a surfboard, it has several benefits. The equipment is small, cheap and allows easy access to all beaches. It also offers easy manoeuvrability in waves (in comparison to a jet-ski).

Rip currents were observed during the field measurements in Vitemölla on September 17-18. The speed of the current is sufficient enough to be a hazard to the public and the current was also possible of carrying the drifter offshore to a distance of about 150m. In most cases, the drifter returned to the beach but a surf zone exit was also found. The rip currents were found to appear with a regular spacing of about 200m, which corresponds well to the beach cusp wavelength noticed on the field visit on March 4. The experiment at Vitemölla on April 26 also showed single events of offshore directed flows, but the data from that particular field measurement is of low quality. Since Haväng resemble Vitemölla, it can be assumed that this beach would have similar current conditions. Knäbäckshusen also have enough longshore morphology variation to possibly induce rip currents.

The velocities from the two first experiments (Sandhammaren April 7 and Vitemölla April 26) are surprisingly high in comparison with literature. Figure 28 indicates that the current velocities for the latter experiment reached above 1.4 m/s, which is significantly stronger than the 0.2 - 1 m/s from earlier studies (Winter et al. (2011), Dalrymple et al. (2011), Short (1985)). During the experiment at Knäbäckshusen on May 31 the velocities are significantly lower. This could partly be explained by the fact that the wave height was somewhat lower but mainly by the fact that the wind during that experiment was very light. It therefore seems like the local wind has a large influence on the current velocities.

8.2 Morphodynamics

The beaches of Haväng, Vitemölla and Knäbäckshusen were found to be the most dynamic beaches through evaluation of old photos but also by the complementary bathymetry measurements (Figure 21). Contrastingly, Södra Vik, Våhallarna and Tobisvik seem to have a rather stationary appearance, even though Tobisvik was found to have a retreating shoreline (see Table 4). The complementary bathymetry measurements would ideally reach further from shore but the field work was limited by not having any accessible boat. The wave modeling show that beaches north of Simrishamn have very similar wave climate except from the fact that Haväng and Vitemölla are somewhat more sheltered from waves propagating from SE. The most prevalent wave direction on these beaches is from NE which partly explains the skewed shape of the bars (see Figure 9 and 10).

It is a reasonable explanation that the great difference in morphology of the beaches relates to the available material at respective site. The sediment is exclusively post-glacial and in this kind of regions, the material is often varied on a small spatial scale. It is well known in literature that foreshore slope is related to grain size and this was also evident from the analysis at the study area. As fine sediments are more mobile, it could be assumed that beaches with smaller

grain size are more prior to be dynamic. This is seemingly the case for Haväng, Vitemölla and Knäbäckshusen which all have medium grain sizes in the range of 0.290 - 0.358 mm. The reason why Knäbäckshusen have a retreating shoreline can further be explained by the fact that the backshore mainly consists of clay or silt which is easily lost offshore during storms. Due to the lack of access to the bathymetry of the three southernmost beaches, any conclusions about the beach profile evolution during the last years is left unanswered. On the other hand, the dunes on these beaches have been shown to accumulate (Persson et al., 2014) as can be seen in Table 4. This region is known to receive a large amount of fine sediment from the South Coast. The accumulation is probably due to large aeolian transport of this fine sediment onto the dunes by the common south-westerly winds (see Figure 14a).

8.3 Numerical Modelling of Nearshore Wave Transformation

In general, EBED is a powerful tool to investigate the driving forces behind rip currents. However, without combining the EBED model with current equations and water levels, it is not possible to locate specific rip current cells to compare with the field data. It should be noted that the wave input at the offshore boundary is considered to have deep water characteristics (which often implies 20 m water depth), but the depth at this boundary is much lower than this. It could thus be assumed that the waves at this location already have been subject to transformation. Since the model after all is used only to attain a schematic overview, this source of error is accepted. Further it can be discussed if it is reasonable to have one input wave along the entire offshore boundary of the EBED grid. For large grids, this would definitely introduce large uncertainty. However, the grid size in this case is relatively small and when taking into account that the offshore wave climate is hindcasted in a rather coarse manner, the applied boundary conditions seem reasonable. Local mean sea water elevation was not be accounted for due to the lack of beach topography data.

SPM-MF is a simple and fast method of hindcasting the wave conditions but it also has some flaws. It was found during the field measurements that the model sometimes overestimates the wave decay. The waves thus seem to decrease in size faster in the model than in reality. The model also assumes that wave direction directly follows the wind direction (unless the direction change between subsequent time steps is larger than 90°). Since the current direction in the model by Longuet-Higgins directly relies on the wave direction, this could give rise to substantial errors.

Anyway, the main issue with the modeling in this project is definitely that the

bathymetric data is outdated. The report by Persson et al. (2014) and the bathymetric survey conducted conclude that most beaches are very dynamic. The use of SGU:s bathymetric data therefore yields large uncertainties in the modeling. However, it could be concluded that the driving forces for rip currents are present in some areas, which could further be validated by the field measurements.

8.4 Safety Recommendations

"*Unawareness is dangerous. Not water.*" (quote by Anders Wernesten, Vattensäkerhet 2016) is a good phrase to keep in mind when dealing with swimming safety. The study of documented rescue missions by SSRS, in combination with in-field observations and lifeguard recommendations from high-risk beaches abroad, is a good starting point for developing guidelines for the local beaches. Below follows some general advice when visiting the beaches in South Eastern Scania.

Haväng, *Vitemölla* and *Knäbäckshusen* have potential of inducing offshore flows which can be hazardous to swimmers. Field investigations showed that the currents can be strong. Even if the current most often carry the swimmer back to shore, it was found that it can also take the swimmer out of the surf zone. The general recommendation would be to stay out of the water when waves are present at the beach. If you get caught in a current: relax and let the current carry you back to shore. If you are carried out of the surf zone, swim parallel to the beach and then try to get back up in a region with breaking waves. At some times it can also be good to swim parallel to the beach when you are in the rip neck to avoid getting carried to far offshore. Attention should also be payed to the longshore currents in the feeder.

Södra Vik, *Vårhallarna* and *Tobisvik* are steep beaches and the waves can often be strong and plunging close to the beach. This can potentially cause the swimmer to have trouble getting up from the water due to the strong backwash. Combined with the coarse sand (hard to get a good foot grip) and steep beach profiles, elderly and children are especially vulnerable. At the corners of the beach where the headland starts, it is possible to assume that rip currents can form and therefore it is important to be extra aware in these parts of the beach. Therefore, avoiding these beaches during high surf is recommended.

Sandhammaren, *Mälarhusen* and *Kyhl* most often induce strong longshore currents during days with onshore or sideshore wind. The data compilation from SSRS data show that accidents are most prevalent on these beaches. The currents can be very strong and quickly carry swimmers along shore. These currents should be escaped by swimming straight towards the beach, but during high surf,

these waters should also be avoided.

To visually present the current condition in the study area, a coarse current map was developed (Figure 42). The map was created on basis of field experiments, bathymetry surveys and theory. No drifter experiments were performed at the beaches around Tobisvik and Vårhallarna simply because the equipment is too sensitive to the violently plunging waves and sharp cliffs. Based on theory it is assumed that rip currents in the proximity of the headlands (like around the jetty in Figure 4c) can develop.

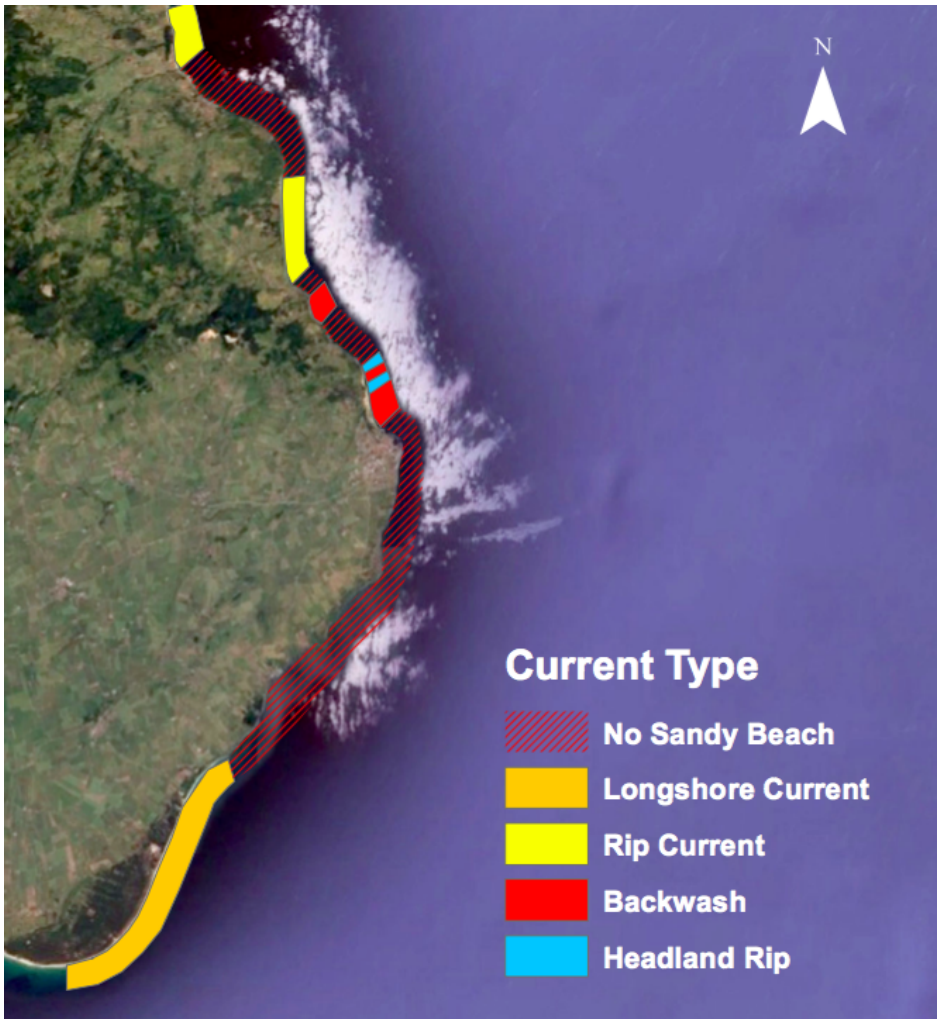

Figure 42: Schematic current map of the study area. Graphics: Google Earth 2016

8.4.1 Warning System

Rip current models and warning systems are tricky to run in real time, especially at dynamic beaches where the bathymetry can change in days or even hours. During the Haväng accident in August 2015, rescue personnel intensely searched

in the surrounding waters. They planned their search with help from a local fisherman that had good knowledge about the prevailing current directions (Claes Jeppson, 2016). Since the currents observed by drifter measurements generally were meandering longshore currents, a simple current model could be a useful tool to visualize in which direction the longshore current is expected to flow. With observed wind speed and direction as input, such a model could be a useful tool for coastal rescue services. The search area could probably be decreased and the possibilities of finding people in the water could increase. It is though doubtful whether a public current warning system could be applicable to the Southeast Coast of Scania or not. As mentioned in the *Theoretical Background*, these models are very complex and require high quality data to give good output. There is ongoing research on real-time bathymetry estimation by video-camera (Dalrymple et al., 2011) and in combination with installation of wave buoys, a warning system could perhaps be possible to set up also for this stretch of coast. Another substantial problem with developing warning systems is that overestimated risks could have negative effect on swimming attendance (and thus also on the economic revenue of beach-related businesses) whilst underestimated risks could give swimmers a false sense of security. This kind of warning system would thus probably be costful for the municipality and therefore it would be more valuable to employ life guards as an initial step to achieve safer beaches.

8.5 Further Research

Regarding nearshore currents, this stretch of coast is an unexplored area. The field measurements done during this project are the first of its kind in this region and to draw any conclusions about when dangerous currents can appear, much more data is needed. The ideal methodology would be to survey the bathymetry closely in time with the field measurements. The wave modeling with EBED would then be of even greater interest.

Some parts of the study area already suffer from erosion and other parts could possibly do so in the future as the sea level rises. Regular bathymetric surveys could lead to increased understanding of the local beach morphodynamics and also be useful in erosion management.

9 Conclusions

This chapter briefly describes what conclusions can be drawn from the the data compilation and field measurements of this thesis.

- The drifters designed in this thesis proved to be a useful tool for investigating nearshore currents. They were found to be easy to maneuver, sufficiently robust and affordable. The spatial accuracy was enough to map currents on a small scale.

- Most beaches in the study area were found to be very dynamic and the bars to be in constant transformation. The beach state concept by Wright and Short (1984) was found hard to apply since the coast does not receive any long period swells. The bathymetry surveys showed that the three northenmost beaches have changed significantly during the last years.

- It was found that rip currents occur not only on swell dominated beaches but also on beaches exposed to wind waves. Rip current cells with an approximate distance of 200m was found on Vitemölla beach on September 17-18. Rip-neck velocities in the range of 0.4 - 1.1 m/s was observed. The other field measurements showed no clear signs of rip currents but a sometimes strong longshore current (up to 1.4 m/s).

- In this study area, rip currents were found to appear on beaches with irregular bathymetry and rhythmic bars.

- The EBED modeling in Vitemölla showed that a longshore wave height variation is induced in the nearshore as the beach is exposed to waves. Specific locations of rip current cells could not be determined using the model with the provided input.

- In contrast to earlier studies (Dalrymple et al., 2011), the data compilation from SSRS revealed that in the study area, longshore current seem to be the type of current that is most prone to get swimmers in danger.

10 Bibliography

Aagaard, T. and Vinther, N. (2008). Cross-Shore Currents in the Surf Zone: Rips or Undertow? *Journal of Coastal Research*, 243(243):561–570.

Bowen, A. J. (1969). Rip Currents. *Journal of Geophysical Research*, 74(23):5467–5478.

Claes Jeppson, R. (2016). Claes Jeppsson, Presentation at Vattensakerhet 2016.

Dalrymple, R. A. (1978). Rip Currents and Their Causes. *Coastal Engineering - Currents and Causes*, 222(1):1414–1425.

Dalrymple, R. A., MacMahan, J. H., Reniers, A. J., and Nelko, V. (2011). Rip Currents. *Annual Review of Fluid Mechanics*, 43(1):551–581.

Davidson-Arnott, R. (2010). *An Introduction to Coastal Processes and Geomorphology*. Cambridge University Press, Cambridge.

Davis, W. (1925). The "Undertow". *Science*, 62(1593):30–33.

Dean, R. G. and Walton, T. L. (1990). Wave Set-up. *Handbook of Coastal and Ocean Engineering*, 1:635–646.

Guza, R. T. and Inman, D. L. (1975). Edge waves and beach cusps. *Journal of Geophysical Research*, 80(21):2997.

Hanson, H. and Larson, M. (2008). Implications of Extreme Waves and Water Levels in the Southern Baltic Sea. *Journal of Hydraulic Research*, 46(Extra2):292–302.

Helsingborgs Dagblad (2015). Drunkning trots varningsskyltar.

Hubertz, J. M. (1986). Observations of Local Wind Effects on Longshore Currents. *Coastal Engineering*, 10:275–288.

Longuet-Higgins, M. and Stewart, R. (1964). Radiation stresses in water waves; a physical discussion, with applications. *Deep Sea Research and Oceanographic Abstracts*, 11(4):529–562.

MacMahan, J. H., Thornton, E. B., and Reniers, A. J. H. M. (2006). Rip current review. *Coastal Engineering*, 53(2-3):191–208.

Mase, H. (2001). Multi-directional Random Wave Transformation Model Based on Energy Balance Equation. *Coastal Engineering*, 43(04).

Nam, P., Larson, M., Hanson, H., and Hoan, L. X. (2009). A numerical model of nearshore waves, currents, and sediment transport. *Coastal Engineering*, 56(11-12):1084 – 1096.

Narra, P., Coelho, C., and Fonseca, J. (2015). Sediment grain size variation along a cross-shore profile - representative d50. *Journal of Coastal Conservation*, 19(3):307–320.

Olsson, D. (2004). Field Studies of Rip Currents in the Lee of Coastal Structures. *Department of Environmental Engineering*, University(November).

Persson, K. M., Nyberg, J., Ising, J., and Persson, M. (2014). Skånes känsliga stränder – ett geologiskt underlag för kustzons planering och erosionsbedömning. Technical report, SGU.

Sabet, B. S. and Barani, G. A. (2011). Design of small GPS drifters for current measurements in the coastal zone. *Ocean and Coastal Management*, 54(2):158–163.

Schmidt, W., Woodward, B., Millikan, K., Guza, R. T., Raubenheimer, B., and Elgar, S. (2003). A GPS-Tracked Surf Zone Drifter * GPS - Equipped Surfzone Drifter. *Journal of Atmospheric and Oceanic Technology*, 20:1069–1075.

Shepard, F., Emery, K., and LaFond, E. (1941). Rip currents: A process of geological importance. *The Journal of Geology*, 49:337–369.

Shepard, F. and Inman, D. (1950). Nearshore Water Circulation Related to Bottom Topography and Wave Refraction. *Transactions, American Geophysical Union*, 31(2):196–212.

Short, A. D. (1985). Rip-current type, spacing and persistence, Narrabeen Beach, Australia. *Marine Geology*, 65(1-2):47–71.

SMHI (2010). Tides in Swedish Waters.

SMHI (2016). Havsvattenstånd 2016. Technical report, Swedish Metrological and Hydrological Institute.

Soderberg, S. (2016). Interview with Sanna Soderberg, Simrishamn Municipality.

U.S. Army Corps of Engineers (1984). Shore Protection Manual. *Engineer Manual*, 1, Fourth.

U.S. Army Corps of Engineers (2002). Coastal Engineering Manual. *Engineer Manual*, 1100-2-110.

Visser, P. J. (1991). Laboratory measurements of uniform longshore currents. *Coastal Engineering*, 15(5-6):563–593.

Wentworth, C. K. (1922). A Scale of Grade and Class Terms for Clastic Sediments. *The Journal of Geology*, 30(5):377–392.

Winter, G., Ap van Dongeren, de Schipper, M., and van Thiel de Vries, J. (2011). A Field and Numerical Study Into Rip Currents in Wind-Sea Dominated Environments. *Coastal Engineering 2012*, pages 1–10.

Wright, L. (1979). Morphodynamics of Reflective and Dissipative Beach and Inshore Systems: Southeastern Australia. *Marine Geology*, 32:105–140.

Wright, L. D. and Short, A. D. (1984). Morphodynamic variability of surf zones and beaches: A synthesis. *Marine Geology*, 56(1–4):93–118.

Zhiyao, S., Tingting, W., Fumin, X., and Ruijie, L. (2008). A simple formula for predicting settling velocity of sediment particles. *Water Science and Engineering*, 1(1):37–43.

11 Appendix

11.1 Wind Comparision

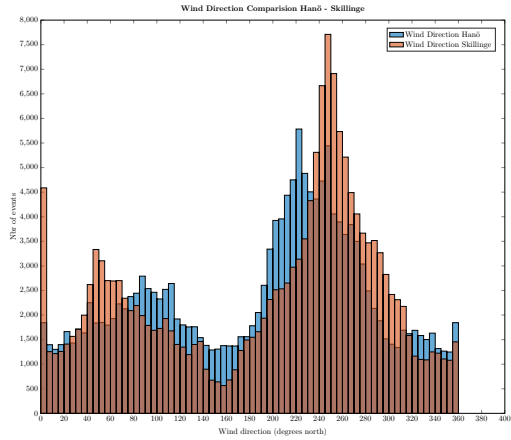

Figure 43: Difference in wind direction between Hanö and Skillinge

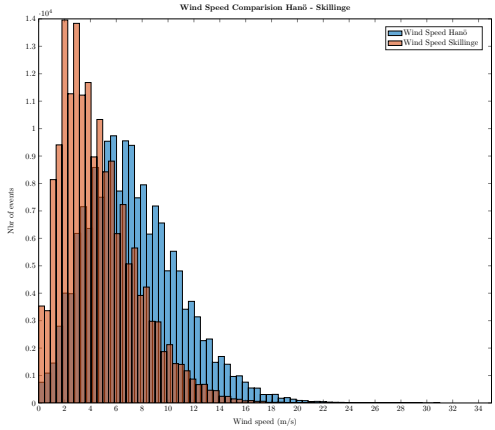

Figure 44: Difference in wind speed between Hanö and Skillinge

11.2 SPM-MF

With the methodology of Hanson and Larson (2008) it is assumed that the waves evolve from existing wave conditions based on an exponential response function:

$$\frac{dH}{dt} = k(H_{eq} - H) \tag{18}$$

where H is the wave height generated by wind, H_{eq} the wave height at equilibrium determined by the SPM-method, t is the duration of the wind and k a response coefficient. The solution to this differential equation is:

$$H = H_{eq} - (H_{eq} - H_{in})exp\left(-\lambda\frac{t}{t_{eq}}\right) \tag{19}$$

where H_{in} is the wave height when new wind conditions start and $\lambda = kt_{eq}$ where t_{eq} is the required time to reach fetch-limited equilibrium conditions. The equations can handle both $H_{eq} > H_{in}$ and $H_{in} < H_{eq}$ which corresponds to wave growth and decay. Hanson and Larson (2008) derived a value of λ by fitting Equation 19 to Equation 24 that is derived as follows (U.S. Army Corps of Engineers, 1984); The time t_M it takes for an area with a defined fetch F and a wind stress factor U_A to reach wave height equilibrium is given as:

$$t_M = 32.15\left(\frac{F^2}{u_A}\right)^{1/3} \tag{20}$$

If the time is less than the time required to reach equilibrium ($t < t_M$) an equivalent fetch F_e can be used in determination of wave height:

$$F_e = \left(\frac{t}{32.15}\right)^{3/2} u_A^{1/2} \tag{21}$$

This equivalent fetch can thus be inserted in the wave height equation for fetch limited conditions:

$$H = 5.112 \cdot 10^{-4} u_A F_e \tag{22}$$

In the same manner, the maximum wave height, only limited by the actual fetch is:

$$H_{max} = 5.112 \cdot 10^{-4} u_A F \tag{23}$$

And thus the wave growth can be expressed as:

$$\frac{H}{H_{max}} = \left(\frac{F_e}{F}\right)^{1/2} = \left(\frac{t}{t_M}\right)^{3/4} \tag{24}$$

The optimum for a least-square fit for these equations was found to give $\lambda = 2.17$ (Hanson and Larson, 2008).

11.3 EBED

EBED is a random multi-directional wave transformation model based on energy dissipation by wave breaking and diffraction terms that was developed by Mase (2001). The energy balance equation with diffraction and energy dissipation is written:

$$\frac{\partial(v_x S)}{\partial x} + \frac{\partial(v_y S)}{\partial y} + \frac{\partial(v_\theta S)}{\partial \theta} =$$

$$\frac{\kappa}{2\omega}\left\{(CC_g cos^2\theta S_y)_y - \frac{1}{2}CC_g cosr\theta S_{yy}\right\}\epsilon_b S \tag{25}$$

The coordinate direction in EBED is set so that the x- and y-direction represents longshore- and cross-shore-directions respectively. θ is the angle measured counter-clockwise from the x-axis and S is the angular-frequency spectrum density. C, C_g are the phase speed and group speed of the waves, ω is the angular frequency and κ is an free parameter used to alternate the effects of diffraction. v_x, v_y, v_θ are the propagation velocities in respective direction given by:

$$\{v_x,\ v_y,\ v_\theta\} = \left\{C_g cos\theta,\ C_g sin\theta,\ \frac{C_g}{C}\left(sin\theta\frac{\partial C}{\partial x} - cos\theta\frac{\partial C}{\partial y}\right)\right\} \tag{26}$$

The first term on the right hand side on Equation 25 is introduced to represent the diffraction effects. The second term describes energy dissipation under wave breaking and ϵ_b is a dissipation coefficient.

This model has proven to be stable even when applied on complex bathymetry. Howerver, the model has shown to overestimate the wave height in the surf zone compared to observations. The overestimation was found to in large extent originate from the algorithm describing energy dissipation due to wave breaking. In order to improve the model's predictive capacity in the surf zone, Nam et al. (2009) proposed a new, modified energy balance equation:

$$\frac{\partial(v_x S)}{\partial x} + \frac{\partial(v_y S)}{\partial y} + \frac{\partial(v_\theta S)}{\partial \theta} =$$

$$\frac{\kappa}{2\omega}\left\{(CC_g cos^2\theta S_y)_y - \frac{1}{2}CC_g cos^2\theta S_{yy}\right\} - \frac{K}{h}C_g(S - S_{stab}) \tag{27}$$

κ is a dimensionless decay coefficient and h is the still water depth. S_{stab} is the stable wave spectrum density which ultimately is a function of the stable wave height ($H_{stab} = \Gamma h$) where Γ is a dimensionless empirical coefficient. When assumed that spectrum density S_S and stable spectrum density S_{stab} are functions of H_s^2 and H_{stab}^2 respectively, the dissipatation term (final term on the right hand

side) in Equation 27 can be replaced by:

$$D_{diss} = \frac{K}{h} = C_g S\left[1 - \frac{\Gamma h}{H_s}^2\right] \tag{28}$$

In this modified-EBED, the value for Γ was modified for the model to fit observed data well, and was finally established to:

$$\Gamma = 0.45, K = \frac{3}{8}(0.3 - 19.2s) \qquad s < 0$$

$$\Gamma = 0.45 + 1.5s, K = \frac{3}{8}(0.3 - 0.5s) \qquad s \geq 0 \tag{29}$$

with s being the bottom slope. The output from the model is three parameters for each cell: significant wave height H_s, significant wave period T_s and mean wave direction $\bar{\theta}$.